Theory of the Muonic Hydrogen Hyperfine Splitting

— Hadronic Corrections —

Franziska Hagelstein (JGU Mainz & PSI Villigen)

in collaboration with

V. Lensky (JGU Mainz)

Hadronic Corrections

Polarizability, Finite Size, Vacuum Polarization ...

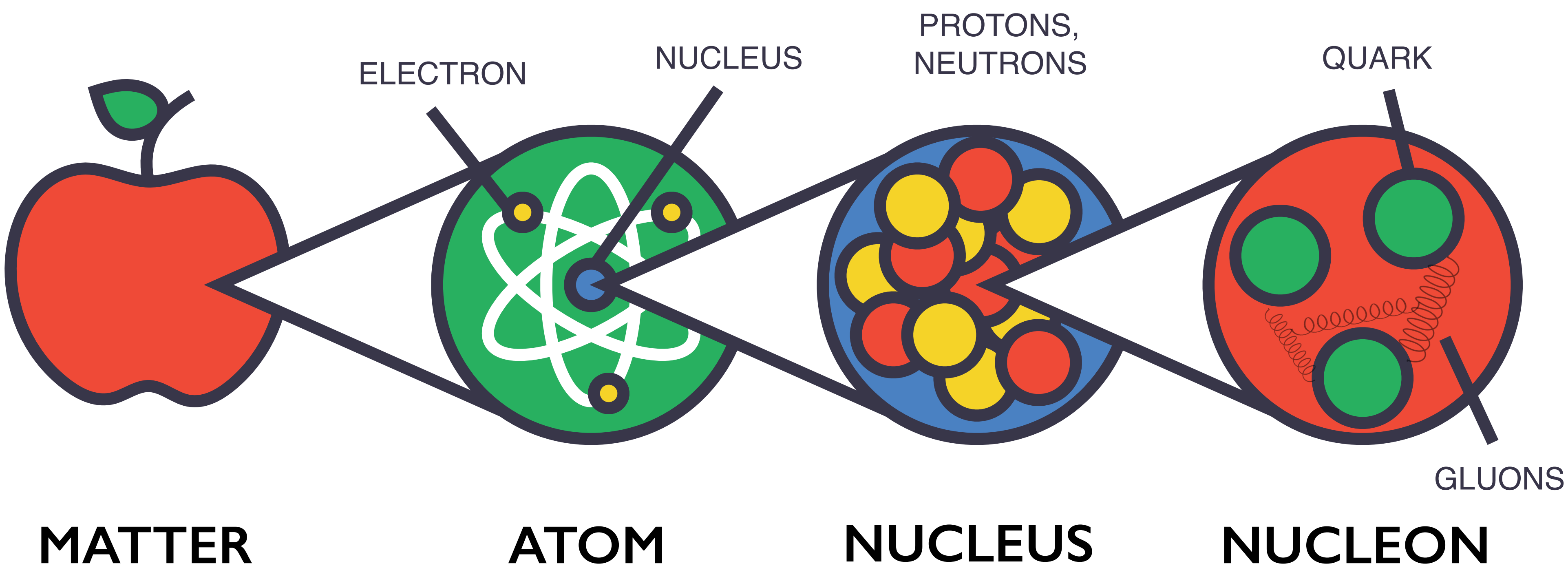

… needed to interpret spectroscopy experiment

… limit the uncertainty of SM predictions

… require careful assessment of uncertainties

Muonic-Hydrogen Spectroscopy

Proton Charge Radius from Lamb Shift

- Accurate extraction of the proton charge radius with unprecedented precision

Muonic-Hydrogen Spectroscopy

Proton Charge Radius from Lamb Shift

- Accurate extraction of the proton charge radius with unprecedented precision
- Comparison of precision measurement and theory prediction:
  - Theory: $E_{\mathrm{LS}}^{(\mathrm{th.})} = \left[206.034\,4(3) - 5.225\,9\,\left(R_E/\mathrm{fm}\right)^2 \right] \mathrm{meV} + E_{\mathrm{LS}}^{(\mathrm{strong})}$

QED
point nucleus

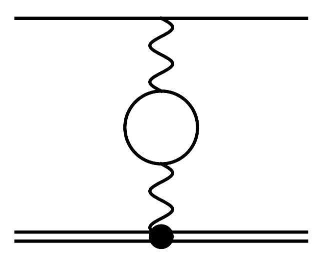

$(Z\alpha)^4$	r_C^2	
$\alpha\,(Z\alpha)^4$	$\mathrm{eVP}^{(1)}$	with r_C^2
$\alpha^2(Z\alpha)^4$	$\mathrm{eVP}^{(2)}$	with r_C^2

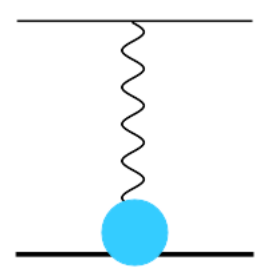

$(Z\alpha)^5$	TPE
$\alpha^2(Z\alpha)^4$	Coulomb distortion
$(Z\alpha)^6$	3PE
$\alpha\,(Z\alpha)^5$	$\mathrm{eVP}^{(1)}$ with TPE
$\alpha\,(Z\alpha)^5$	$\mu\mathrm{SE}^{(1)} + \mu\mathrm{VP}^{(1)}$ with TPE

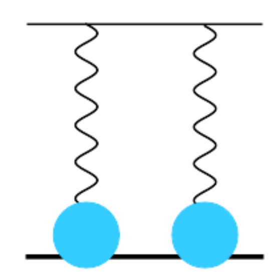

[Pachucki et al., Rev. Mod. Phys. 96 (2024) 015001]

Muonic-Hydrogen Spectroscopy

Proton Charge Radius from Lamb Shift

- Accurate extraction of the proton charge radius with unprecedented precision
- Comparison of precision measurement and theory prediction:
  - Theory: $E_{\mathrm{LS}}^{(\mathrm{th.})} = \left[206.0344(3) - 5.2259\,\left(R_E/\mathrm{fm}\right)^2\right]\mathrm{meV} + E_{\mathrm{LS}}^{(\mathrm{strong})}$
  - Experiment: $E_{\mathrm{LS}}^{(\mathrm{exp.})} = 202.3706(23)\,\mathrm{meV}$

[μeV]	E	ΔE	ΔE /E
Lamb shift	202 370.6	2.3	10^{-5}
2S HFS	22 808.9	5.1	2×10^{-4}

[CREMA Collaboration (2010/2013)]

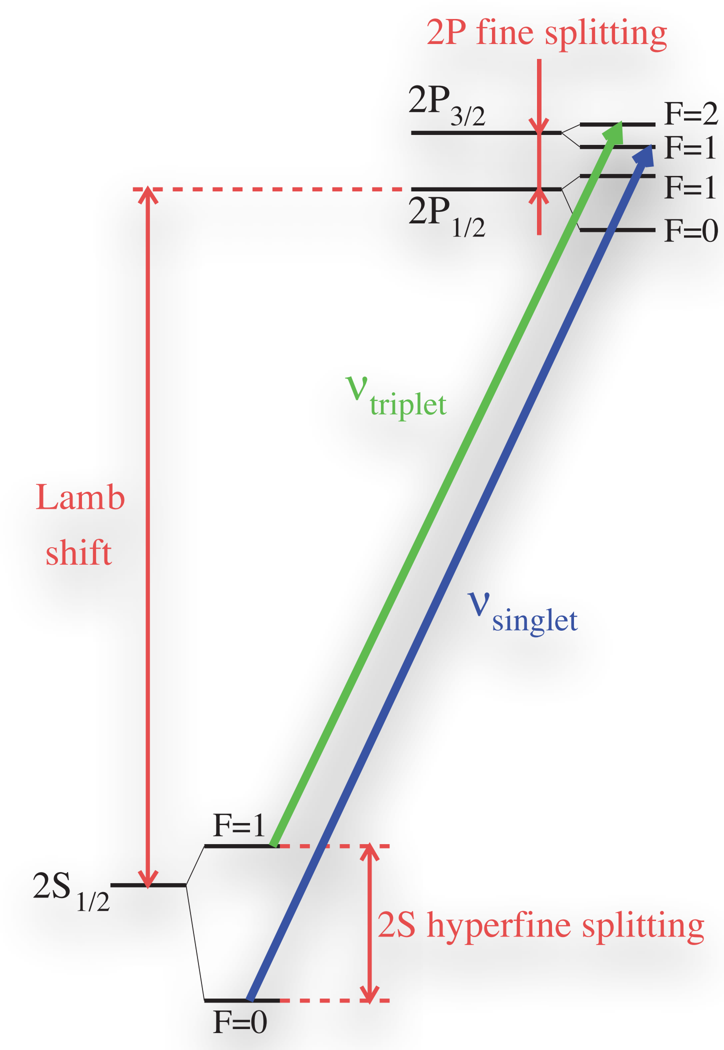

Muonic-Hydrogen Spectroscopy

Proton Charge Radius from Lamb Shift

- Accurate extraction of the proton charge radius with unprecedented precision
- Comparison of precision measurement and theory prediction:
  - Theory: $E_{\mathrm{LS}}^{(\mathrm{th.})} = \left[206.034\,4(3) - 5.225\,9\ \left(R_E/\mathrm{fm}\right)^2\right]\mathrm{meV} + E_{\mathrm{LS}}^{(\mathrm{strong})}$
  - Experiment: $E_{\mathrm{LS}}^{(\mathrm{exp.})} = 202.370\,6(23)\,\mathrm{meV}$

[μeV]	E	ΔE	ΔE /E
Lamb shift	202 370.6	2.3	10^{-5}
2S HFS	22 808.9	5.1	2×10^{-4}
1S HFS	~ 182 626(5)	~ 0.02	10^{-6} to 10^{-7}

[CREMA Collaboration (2010/2013)]

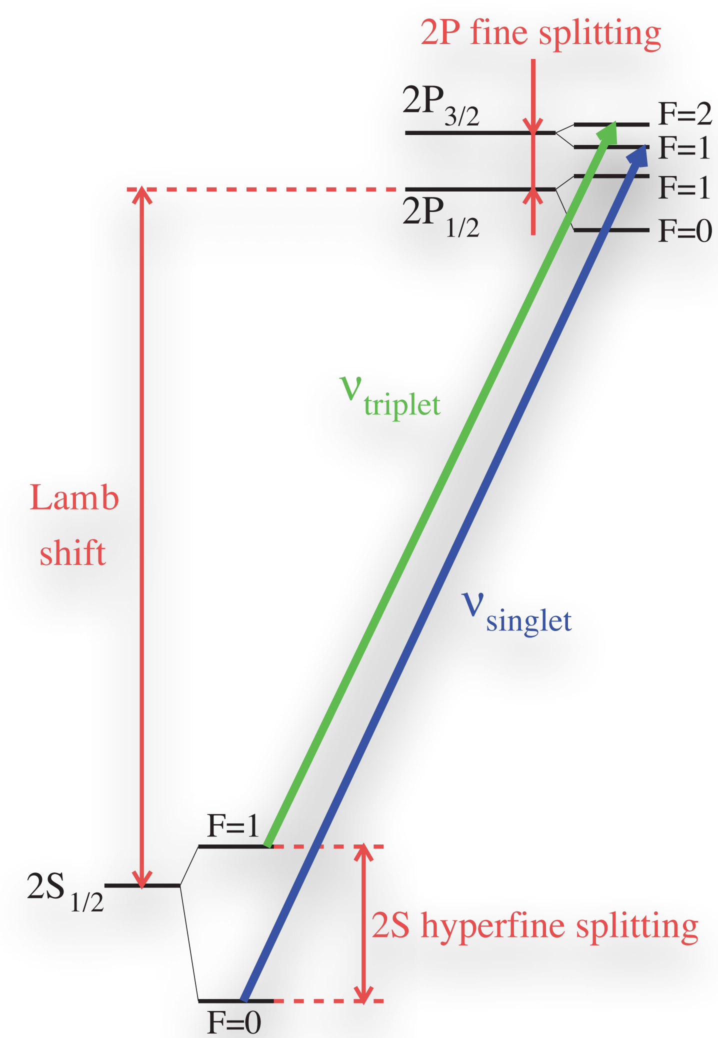

Muonic-Hydrogen Spectroscopy

1S Hyperfine Splitting

- Measurements of the μH ground-state HFS planned by two independent collaborations:
  - CREMA coll. aims at 10^{-7} accuracy
    [talks by Randolf Pohl and Siddharth Rajamohanan]
    CREMA, Nature 466 (2010) 213 - 216
    CREMA, Science 339 (2013) 417–420
  - First run by FAMU coll. in 2023/2024
    [poster by Eugenio Fasci]
    FAMU, EPJ A 61 (2025) 12, 284
- Theory predictions for HFS in μH are driven by 1S HFS in H
  [poster by Andrzej Maroń and talk by K. Pachucki]
  A. Maroń, M. Pańtak and K. Pachucki, 2604.06930
  [talk by V. Pascalutsa]
  A. Antognini, FH, V. Pascalutsa, Ann. Rev. Nucl. Part. 72 (2022)

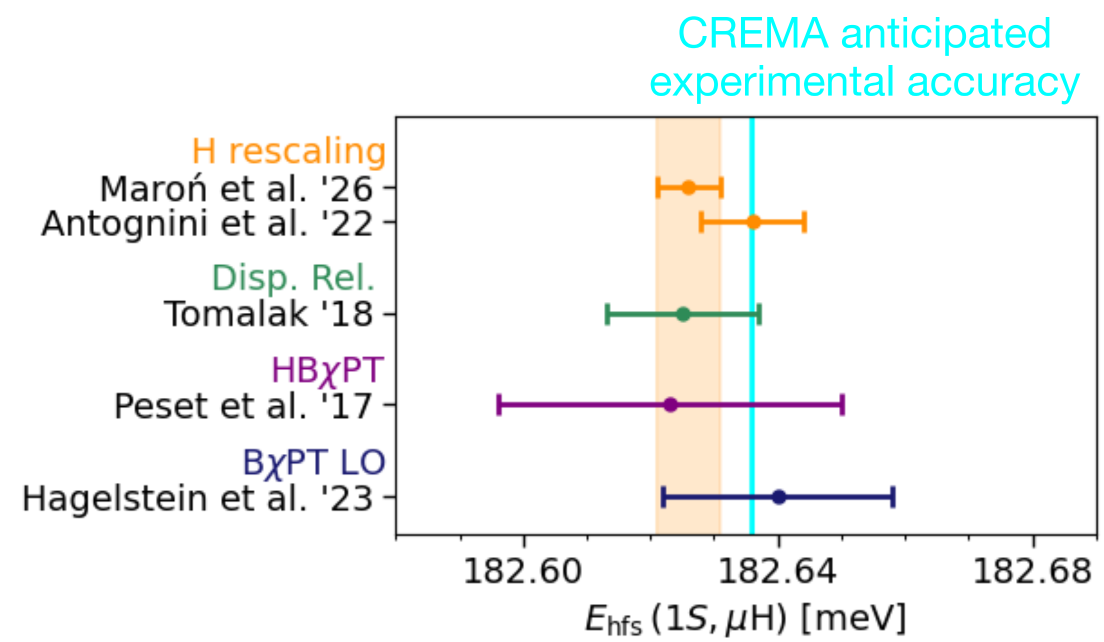

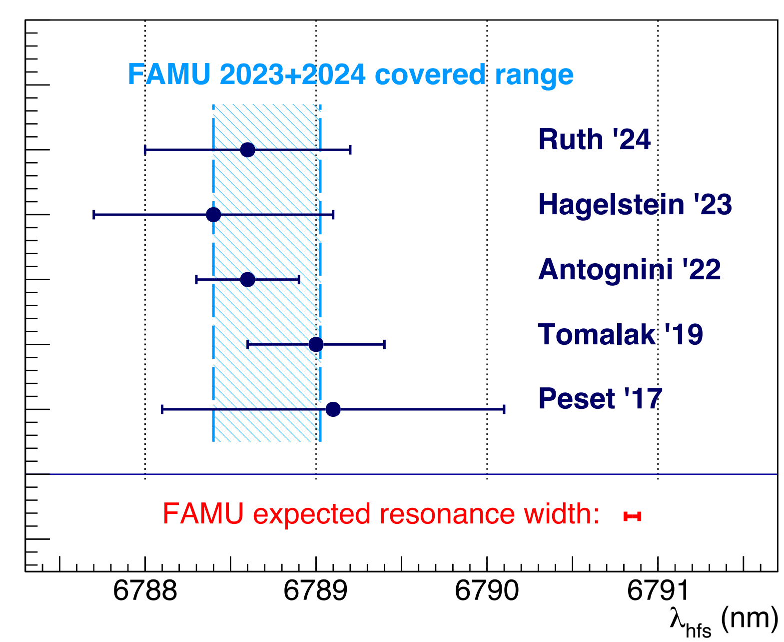

Proton Zemach Radius

From 1S Hyperfine Splitting in μH

The hyperfine splitting of μH (theory update):

A. Antognini, FH, V. Pascalutsa, Ann. Rev. Nucl. Part. **72** (2022)

$$E_{1S\text{-hfs}} = \Big[\underbrace{182.443}_{E_\mathrm{F}} \underbrace{+1.350(7)}_{\mathrm{QED+weak}} \underbrace{+0.004}_{\mathrm{hVP}} \underbrace{-1.30653(17)\left(\frac{r_{\mathrm{Z}p}}{\mathrm{fm}}\right) + E_\mathrm{F}\left(1.01656(4)\,\Delta_\mathrm{recoil} + 1.00402\,\Delta_\mathrm{pol}\right)}_{2\gamma\ \mathrm{incl.\ radiative\ corr.}}\Big]\,\mathrm{meV}$$

measure

Proton Zemach Radius

From 1S Hyperfine Splitting in μH

The hyperfine splitting of μH (theory update):

A. Antognini, FH, V. Pascalutsa, Ann. Rev. Nucl. Part. **72** (2022)

$$E_{1S\text{-hfs}} = \Big[\underbrace{182.443}_{E_\mathrm{F}} \underbrace{+1.350(7)}_{\text{QED+weak}} \underbrace{+0.004}_{\text{hVP}} \underbrace{-1.30653(17)\left(\frac{r_{\mathrm{Z}p}}{\mathrm{fm}}\right) + E_\mathrm{F}\left(1.01656(4)\,\Delta_\mathrm{recoil} + 1.00402\,\Delta_\mathrm{pol}\right)}_{2\gamma \text{ incl. radiative corr.}}\Big]\,\mathrm{meV}$$

measure

extract

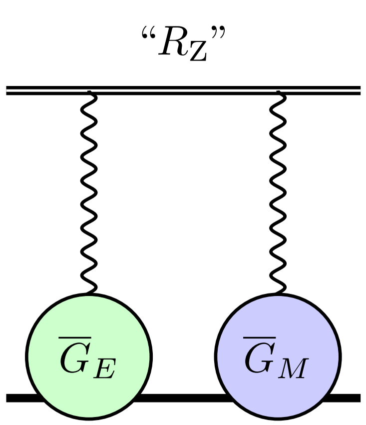

$$R_\mathrm{Z} \equiv \int \mathrm{d}\boldsymbol{r}\, r \int \mathrm{d}\boldsymbol{r}'\, \varrho_E(|\boldsymbol{r}' - \boldsymbol{r}|)\, \varrho_M(\boldsymbol{r}')$$
$$= -\frac{4}{\pi}\int_0^\infty \frac{\mathrm{d}Q}{Q^2}\left[\frac{G_E(Q^2)G_M(Q^2)}{1+\kappa} - 1\right]$$

Zemach radius can help to pin down the magnetic properties of the proton

Theory prediction

Limited by Hadronic Corrections

HFS = QED + weak + hadronic

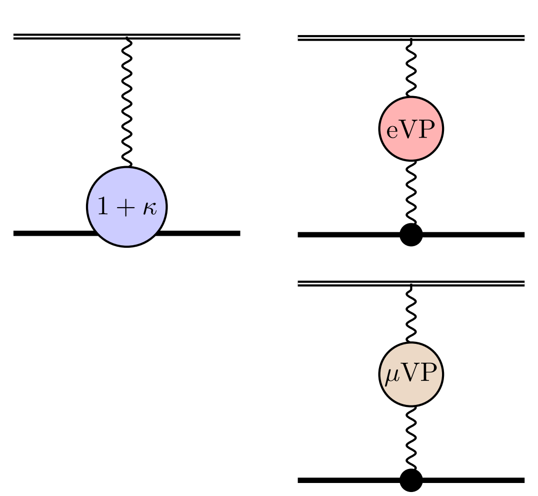

Theory prediction

Limited by Hadronic Corrections

HFS = QED + weak + hadronic

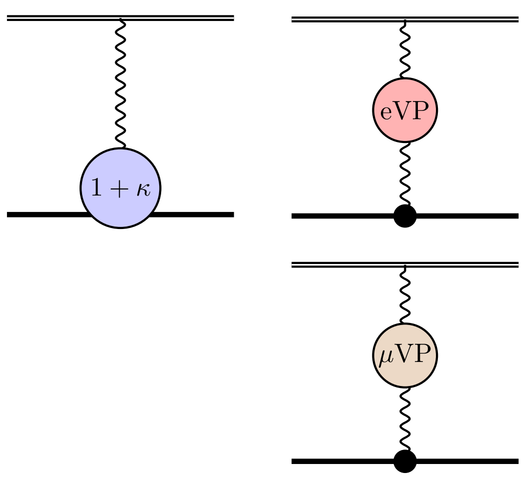

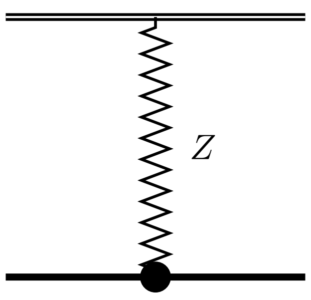

Theory prediction

Limited by Hadronic Corrections

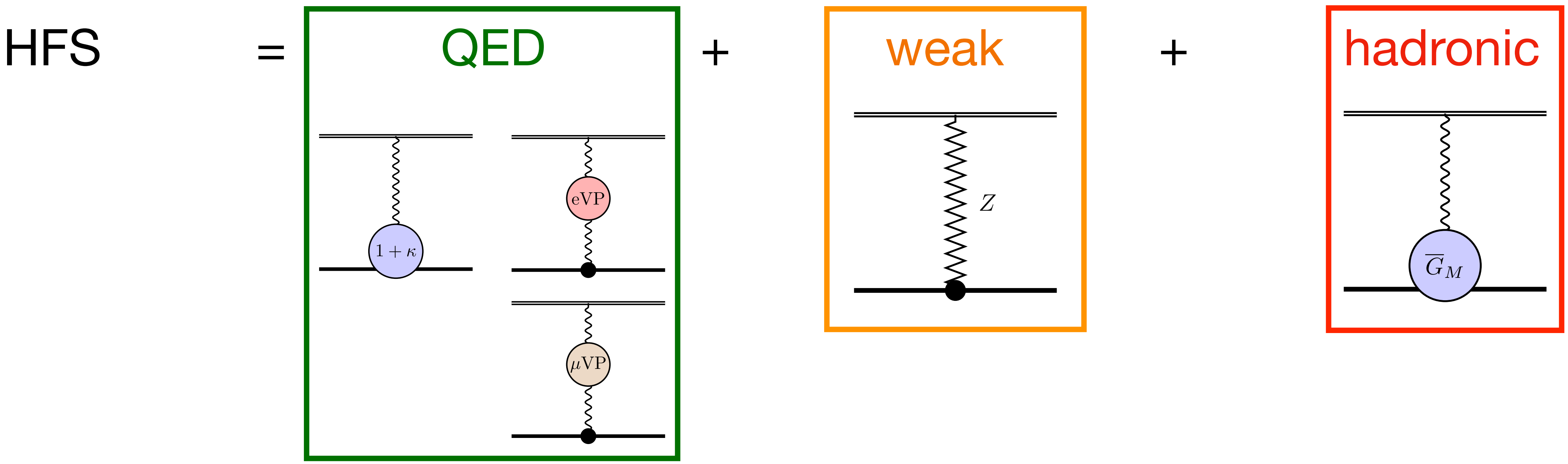

hadronic = HVP + Zemach radius + finite-size recoil + polarizability

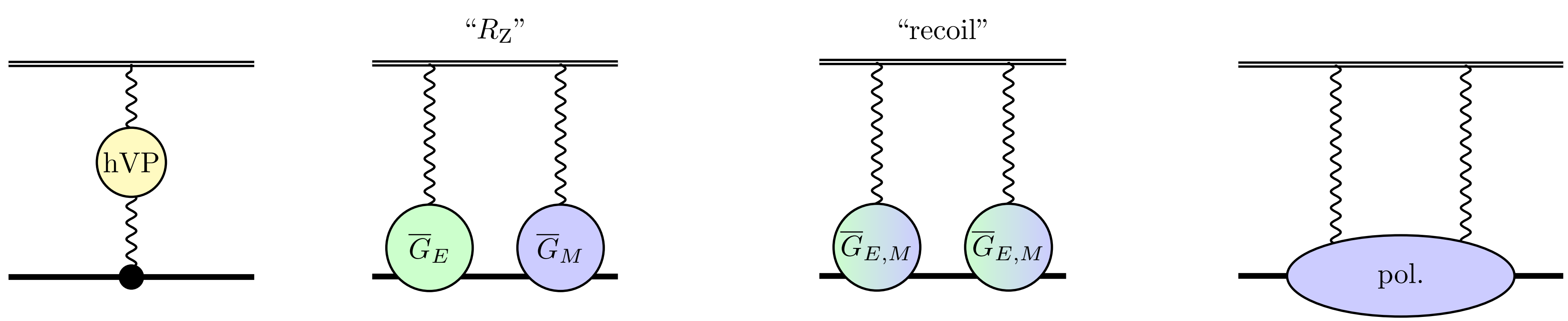

Empirical Refinement

Hydrogen Rescaling

A. Maroń, et al., 2604.06930

TABLE I. Contributions to HFS in μH, constants from Ref. [19], $g_p = 5.585\,694\,6893(16)$, $\nu_F = 44\,114\,600.4(2.0)$ MHz, $E_F = 0.182\,443\,32\,8(8)$ eV, a_μ is the muon magnetic moment anomaly.

Term	Value	Reference
a_μ	0.001 165 92	Ref. [19]
$(1+a_\mu)\,\delta^{(1)}_{\rm evp}$	0.006 082 37	Eq. (15)
$(1+a_\mu)\,\delta^{(2)}_{\rm evp}$	0.000 061 32	Eq. (18)
$\delta^{(2)}$	−0.000 016 34	Eq. (91), Ref.[15]
$\delta^{(3)}$	−0.000 007 10	Eq. (92), Ref.[15, 20]
$\delta^{(3)}_{\rm rel,evp}$	0.000 001 15	Eq. (33)
$\delta^{(3)}_{\mu{\rm vp,evp}}$	0.000 001 17	Eq. (87)
$\delta^{(3)}_{\rm se,evp1}$	−0.000 001 70	Eq. (89)
$\delta^{(3)}_{\rm se,evp2}$	0.000 000(2)	EVP on muon line
$\delta^{(1)}_{\rm fns}$	−0.008 237(21)	Eqs. (93,94), Ref.[21]
$\delta^{(1)}_{\rm rec}$	0.001 672(3)	Eq. (95), Ref.[17]
$\delta^{(1)}_{\rm pol}$	0.000 200 6(52 4)	Eq. (96), Ref.[22]
$\frac{\alpha}{\pi}\,c_1\,\delta^{(1)}_{\rm fns}$	−0.000 033 12	Eq. (97)
$\frac{\alpha}{\pi}\,c_1\,\delta^{(1)}_{\rm rec}$	0.000 006 72	Eq. (97)
$\delta^{(2)}_{\rm evp,fns}$	−0.000 149 81	Eq. (65)
$\delta^{(2)}_{\rm evp,rec}$	0.000 025 24	Eq. (66)
$\delta^{(2)}_{\mu{\rm vp,fns}}$	−0.000 025 10	Eq. (70)
$\delta^{(2)}_{\mu{\rm vp,rec}}$	−0.000 001 18	Eq. (71)
$\delta^{(2)}_{\rm se,fns}$	0.000 016 18	Eq. (81)
$\delta^{(2)}_{\rm se,rec}$	0.000 016 48	Eq. (84)
$\delta^{(2)}_{\rm rel,fns}$	−0.000 050 85	Eq. (102), Ref.[23]
$\delta^{(2)}_{\rm rel,rec}$	0.000 118 86	Eq. (103), Ref.[4]
$\delta^{(2)}_{\rm rel,rec2}$	0.000 000(12)	$(Z\,\alpha)^2\,(m/M)^2$
$\delta^{(2)}_{\rm rel,rec,fns}$	0.000 000(12)	$(Z\,\alpha)^2\,m^2/M\,r_Z$
$\delta^{(2)}_{\rm hvp}$	0.000 011 80(8)	Eq. (104), Ref. [24]
$\delta^{(3)}_{\rm fns}$	0.000 000(2)	$\alpha^3\,m\,r_Z$
$\delta_{\rm weak}$	0.000 011 99	Eq. (105)
δ	0.000 870 (60)	total value

Empirical Refinement

Hydrogen Rescaling

A. Maroń, et al., 2604.06930

TABLE I. Contributions to HFS in μH, constants from Ref. [19], $g_p = 5.585\,694\,6893(16)$, $\nu_F = 44\,114\,600.4(2.0)$ MHz, $E_F = 0.182\,443\,32\,8(8)$ eV, a_μ is the muon magnetic moment anomaly.

Term	Value	Reference
a_μ	0.001 165 92	Ref. [19]
$(1+a_\mu)\,\delta^{(1)}_{\rm evp}$	0.006 082 37	Eq. (15)
$(1+a_\mu)\,\delta^{(2)}_{\rm evp}$	0.000 061 32	Eq. (18)
$\delta^{(2)}$	−0.000 016 34	Eq. (91), Ref.[15]
$\delta^{(3)}$	−0.000 007 10	Eq. (92), Ref.[15, 20]
$\delta^{(3)}_{\rm rel,evp}$	0.000 001 15	Eq. (33)
$\delta^{(3)}_{\mu{\rm vp,evp}}$	0.000 001 17	Eq. (87)
$\delta^{(3)}_{\rm se,evp1}$	−0.000 001 70	Eq. (89)
$\delta^{(3)}_{\rm se,evp2}$	0.000 000(2)	EVP on muon line
$\delta^{(1)}_{\rm fns}$	−0.008 237(21)	Eqs. (93,94), Ref.[21]
$\delta^{(1)}_{\rm rec}$	0.001 672(3)	Eq. (95), Ref.[17]
$\delta^{(1)}_{\rm pol}$	0.000 200 6(52 4)	Eq. (96), Ref.[22]
$\frac{\alpha}{\pi}\,c_1\,\delta^{(1)}_{\rm fns}$	−0.000 033 12	Eq. (97)
$\frac{\alpha}{\pi}\,c_1\,\delta^{(1)}_{\rm rec}$	0.000 006 72	Eq. (97)
$\delta^{(2)}_{\rm evp,fns}$	−0.000 149 81	Eq. (65)
$\delta^{(2)}_{\rm evp,rec}$	0.000 025 24	Eq. (66)
$\delta^{(2)}_{\mu{\rm vp,fns}}$	−0.000 025 10	Eq. (70)
$\delta^{(2)}_{\mu{\rm vp,rec}}$	−0.000 001 18	Eq. (71)
$\delta^{(2)}_{\rm se,fns}$	0.000 016 18	Eq. (81)
$\delta^{(2)}_{\rm se,rec}$	0.000 016 48	Eq. (84)
$\delta^{(2)}_{\rm rel,fns}$	−0.000 050 85	Eq. (102), Ref.[23]
$\delta^{(2)}_{\rm rel,rec}$	0.000 118 86	Eq. (103), Ref.[4]
$\delta^{(2)}_{\rm rel,rec2}$	0.000 000(12)	$(Z\,\alpha)^2\,(m/M)^2$
$\delta^{(2)}_{\rm rel,rec,fns}$	0.000 000(12)	$(Z\,\alpha)^2\,m^2/M\,r_Z$
$\delta^{(2)}_{\rm hvp}$	0.000 011 80(8)	Eq. (104), Ref. [24]
$\delta^{(3)}_{\rm fns}$	0.000 000(2)	$\alpha^3\,m\,r_Z$
$\delta_{\rm weak}$	0.000 011 99	Eq. (105)
δ	0.000 870 (60)	total value

- Zemach radius = largest correction

Empirical Refinement

A. Maroń, et al., 2604.06930

Hydrogen Rescaling

TABLE I. Contributions to HFS in μH, constants from Ref. [19], $g_p = 5.585\,694\,6893(16)$, $\nu_F = 44\,114\,600.4(2.0)$ MHz, $E_F = 0.182\,443\,32\,8(8)$ eV, a_μ is the muon magnetic moment anomaly.

Term	Value	Reference
a_μ	0.001 165 92	Ref. [19]
$(1+a_\mu)\,\delta^{(1)}_{\rm evp}$	0.006 082 37	Eq. (15)
$(1+a_\mu)\,\delta^{(2)}_{\rm evp}$	0.000 061 32	Eq. (18)
$\delta^{(2)}$	−0.000 016 34	Eq. (91), Ref.[15]
$\delta^{(3)}$	−0.000 007 10	Eq. (92), Ref.[15, 20]
$\delta^{(3)}_{\rm rel,evp}$	0.000 001 15	Eq. (33)
$\delta^{(3)}_{\mu{\rm vp,evp}}$	0.000 001 17	Eq. (87)
$\delta^{(3)}_{\rm se,evp1}$	−0.000 001 70	Eq. (89)
$\delta^{(3)}_{\rm se,evp2}$	0.000 000(2)	EVP on muon line
$\delta^{(1)}_{\rm fns}$	−0.008 237(21)	Eqs. (93,94), Ref.[21]
$\delta^{(1)}_{\rm rec}$	0.001 672(3)	Eq. (95), Ref.[17]
$\delta^{(1)}_{\rm pol}$	0.000 200 6(52 4)	Eq. (96), Ref.[22]
$\frac{\alpha}{\pi}\,c_1\,\delta^{(1)}_{\rm fns}$	−0.000 033 12	Eq. (97)
$\frac{\alpha}{\pi}\,c_1\,\delta^{(1)}_{\rm rec}$	0.000 006 72	Eq. (97)
$\delta^{(2)}_{\rm evp,fns}$	−0.000 149 81	Eq. (65)
$\delta^{(2)}_{\rm evp,rec}$	0.000 025 24	Eq. (66)
$\delta^{(2)}_{\mu{\rm vp,fns}}$	−0.000 025 10	Eq. (70)
$\delta^{(2)}_{\mu{\rm vp,rec}}$	−0.000 001 18	Eq. (71)
$\delta^{(2)}_{\rm se,fns}$	0.000 016 18	Eq. (81)
$\delta^{(2)}_{\rm se,rec}$	0.000 016 48	Eq. (84)
$\delta^{(2)}_{\rm rel,fns}$	−0.000 050 85	Eq. (102), Ref.[23]
$\delta^{(2)}_{\rm rel,rec}$	0.000 118 86	Eq. (103), Ref.[4]
$\delta^{(2)}_{\rm rel,rec2}$	0.000 000(12)	$(Z\,\alpha)^2\,(m/M)^2$
$\delta^{(2)}_{\rm rel,rec,fns}$	0.000 000(12)	$(Z\,\alpha)^2\,m^2/M\,r_Z$
$\delta^{(2)}_{\rm hvp}$	0.000 011 80(8)	Eq. (104), Ref. [24]
$\delta^{(3)}_{\rm fns}$	0.000 000(2)	$\alpha^3\,m\,r_Z$
$\delta_{\rm weak}$	0.000 011 99	Eq. (105)
δ	0.000 870 (60)	total value

- Zemach radius = largest correction
- Refinement of TPE effects needed

Empirical Refinement

Hydrogen Rescaling

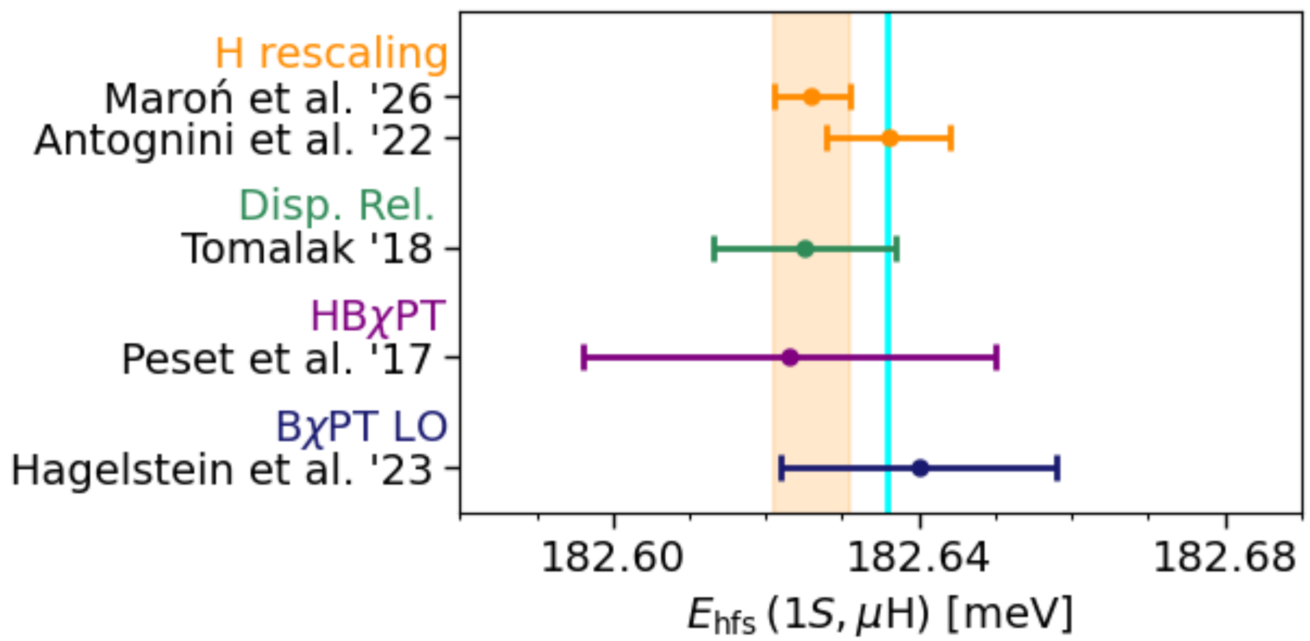

A. Maroń, et al., 2604.06930

δ	0.000 870 (60)	total value
$\frac{m_\mu}{m_e}[\delta_{\rm exp}(\rm H) - \delta(\rm H)]$	0.000 133	Sec. IX
$\delta_{\rm corr}$	0.001 003 (30)	corrected total value

- Zemach radius = largest correction
- Refinement of TPE effects needed
- Understand lepton-mass scaling

A. Maroń, et al., 2604.06930

TABLE I. Contributions to HFS in μH, constants from Ref. [19], $g_p = 5.585\,694\,6893(16)$, $\nu_F = 44\,114\,600.4(2.0)$ MHz, $E_F = 0.182\,443\,32\,8(8)$ eV, a_μ is the muon magnetic moment anomaly.

Term	Value	Reference
a_μ	0.001 165 92	Ref. [19]
$(1+a_\mu)\,\delta^{(1)}_{\rm evp}$	0.006 082 37	Eq. (15)
$(1+a_\mu)\,\delta^{(2)}_{\rm evp}$	0.000 061 32	Eq. (18)
$\delta^{(2)}$	−0.000 016 34	Eq. (91), Ref.[15]
$\delta^{(3)}$	−0.000 007 10	Eq. (92), Ref.[15, 20]
$\delta^{(3)}_{\rm rel,evp}$	0.000 001 15	Eq. (33)
$\delta^{(3)}_{\mu\rm vp,evp}$	0.000 001 17	Eq. (87)
$\delta^{(3)}_{\rm se,evp1}$	−0.000 001 70	Eq. (89)
$\delta^{(3)}_{\rm se,evp2}$	0.000 000(2)	EVP on muon line
$\delta^{(1)}_{\rm fns}$	−0.008 237(21)	Eqs. (93,94), Ref.[21]
$\delta^{(1)}_{\rm rec}$	0.001 672(3)	Eq. (95), Ref.[17]
$\delta^{(1)}_{\rm pol}$	0.000 200 6(52 4)	Eq. (96), Ref.[22]
$\frac{\alpha}{\pi}\,c_1\,\delta^{(1)}_{\rm fns}$	−0.000 033 12	Eq. (97)
$\frac{\alpha}{\pi}\,c_1\,\delta^{(1)}_{\rm rec}$	0.000 006 72	Eq. (97)
$\delta^{(2)}_{\rm evp,fns}$	−0.000 149 81	Eq. (65)
$\delta^{(2)}_{\rm evp,rec}$	0.000 025 24	Eq. (66)
$\delta^{(2)}_{\mu\rm vp,fns}$	−0.000 025 10	Eq. (70)
$\delta^{(2)}_{\mu\rm vp,rec}$	−0.000 001 18	Eq. (71)
$\delta^{(2)}_{\rm se,fns}$	0.000 016 18	Eq. (81)
$\delta^{(2)}_{\rm se,rec}$	0.000 016 48	Eq. (84)
$\delta^{(2)}_{\rm rel,fns}$	−0.000 050 85	Eq. (102), Ref.[23]
$\delta^{(2)}_{\rm rel,rec}$	0.000 118 86	Eq. (103), Ref.[4]
$\delta^{(2)}_{\rm rel,rec2}$	0.000 000(12)	$(Z\alpha)^2\,(m/M)^2$
$\delta^{(2)}_{\rm rel,rec,fns}$	0.000 000(12)	$(Z\alpha)^2\,m^2/M\,r_Z$
$\delta^{(2)}_{\rm hvp}$	0.000 011 80(8)	Eq. (104), Ref. [24]
$\delta^{(3)}_{\rm fns}$	0.000 000(2)	$\alpha^3\,m\,r_Z$
$\delta_{\rm weak}$	0.000 011 99	Eq. (105)
δ	0.000 870 (60)	total value

Lepton-Mass Scaling

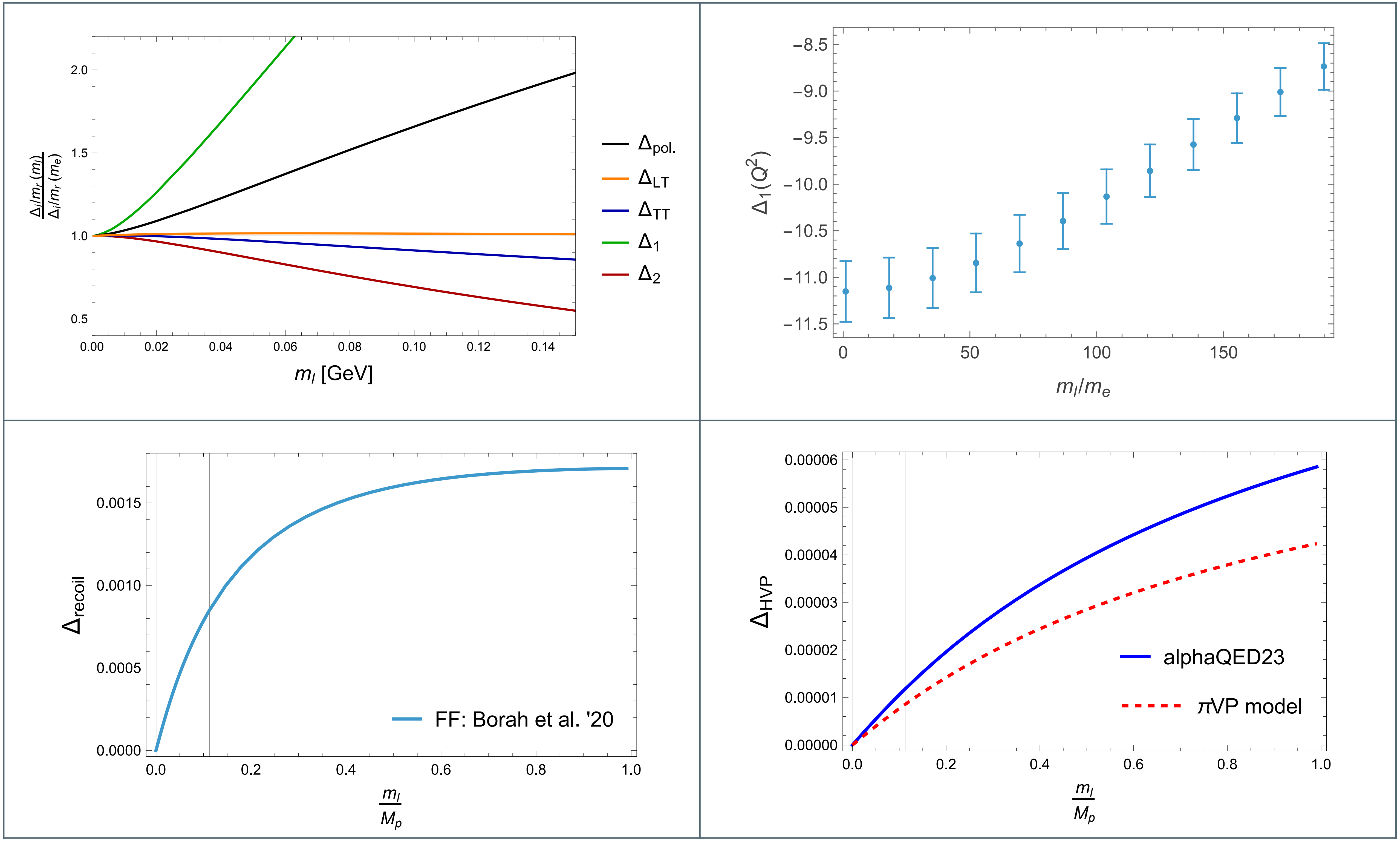

Two-photon exchange (TPE)

Zemach Radius, Recoil, Polarizability

A. Antognini, FH, V. Pascalutsa,
Ann. Rev. Nucl. Part. 72 (2022)

Table 1 Forward 2γ-exchange contribution to the HFS in μH.

Reference	Δ_Z [ppm]	Δ_{recoil} [ppm]	Δ_{pol} [ppm]	Δ_1 [ppm]	Δ_2 [ppm]	$E^{\langle 2\gamma\rangle}_{1S\text{-hfs}}$ [meV]
DATA-DRIVEN						
Pachucki '96 (1)	−8025	1666	0(658)			−1.160
Faustov et al. '01 (9)[a]	−7180		410(80)	468	−58	
Faustov et al. '06 (10)[b]			470(104)	518	−48	
Carlson et al. '11 (11)[c]	−7703	931	351(114)	370(112)	−19(19)	−1.171(39)
Tomalak '18 (12)[d]	−7333(48)	846(6)	364(89)	429(84)	−65(20)	−1.117(19)
HEAVY-BARYON χPT						
Peset et al. '17 (13)						−1.161(20)
LEADING-ORDER χPT						
Hagelstein et al. '16 (14)			37(95)	29(90)	9(29)	
+ $\Delta(1232)$ EXCIT.						
Hagelstein et al. '18 (15)			−13	84	−97	

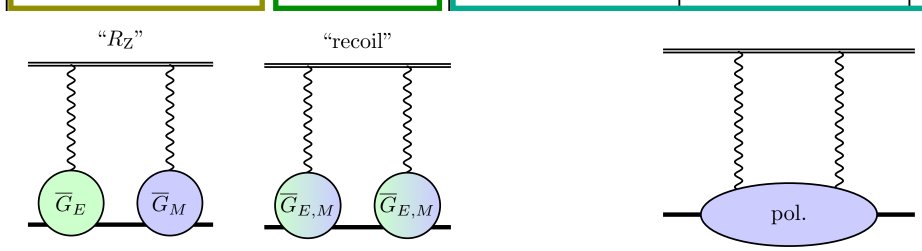

Proton Polarizability

— Inelastic TPE —

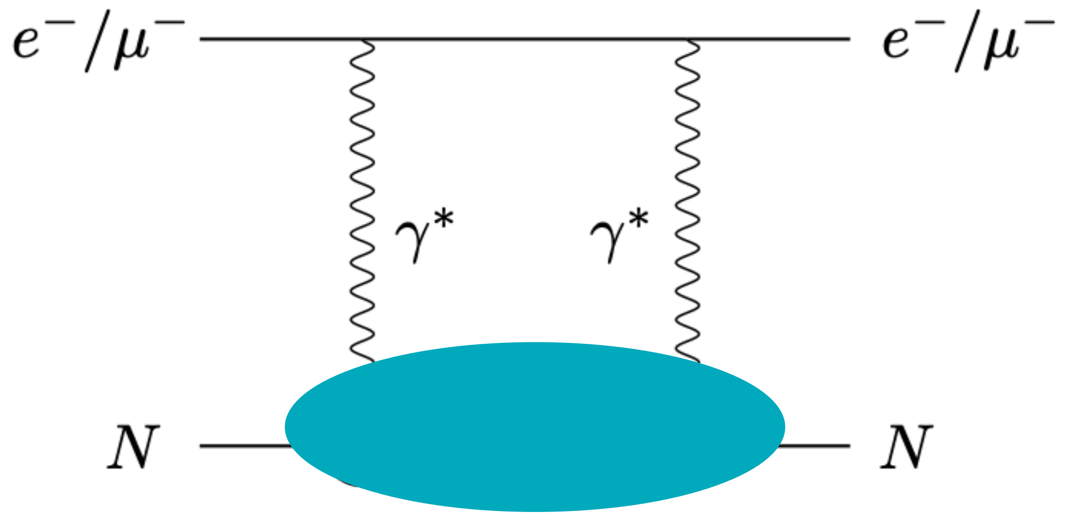

Two-photon exchange (TPE)

Zemach Radius, Recoil, Polarizability

A. Antognini, FH, V. Pascalutsa,
Ann. Rev. Nucl. Part. 72 (2022)

Table 1 Forward 2γ-exchange contribution to the HFS in μH.

Reference	Δ_Z [ppm]	Δ_{recoil} [ppm]	Δ_{pol} [ppm]	Δ_1 [ppm]	Δ_2 [ppm]	$E^{\langle 2\gamma \rangle}_{1S\text{-hfs}}$ [meV]
DATA-DRIVEN						
Pachucki '96 (1)	−8025	1666	0(658)			−1.160
Faustov et al. '01 (9)[a]	−7180		410(80)	468	−58	
Faustov et al. '06 (10)[b]			470(104)	518	−48	
Carlson et al. '11 (11)[c]	−7703	931	351(114)	370(112)	−19(19)	−1.171(39)
Tomalak '18 (12)[d]	−7333(48)	846(6)	364(89)	429(84)	−65(20)	−1.117(19)
HEAVY-BARYON χPT						
Peset et al. '17 (13)						−1.161(20)
LEADING-ORDER χPT						
Hagelstein et al. '16 (14)			37(95)	29(90)	9(29)	
+ $\Delta(1232)$ EXCIT.						
Hagelstein et al. '18 (15)			−13	84	−97	

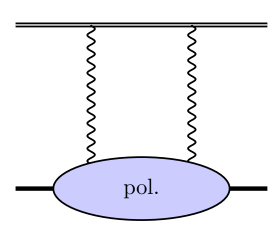

Data-driven dispersive approach

Baryon Chiral Perturbation Theory

Lattice QCD ?

Polarizability Effect

BChPT vs. Data-driven Dispersion Relations

Baryon Chiral Perturbation Theory

Data-driven dispersive approach

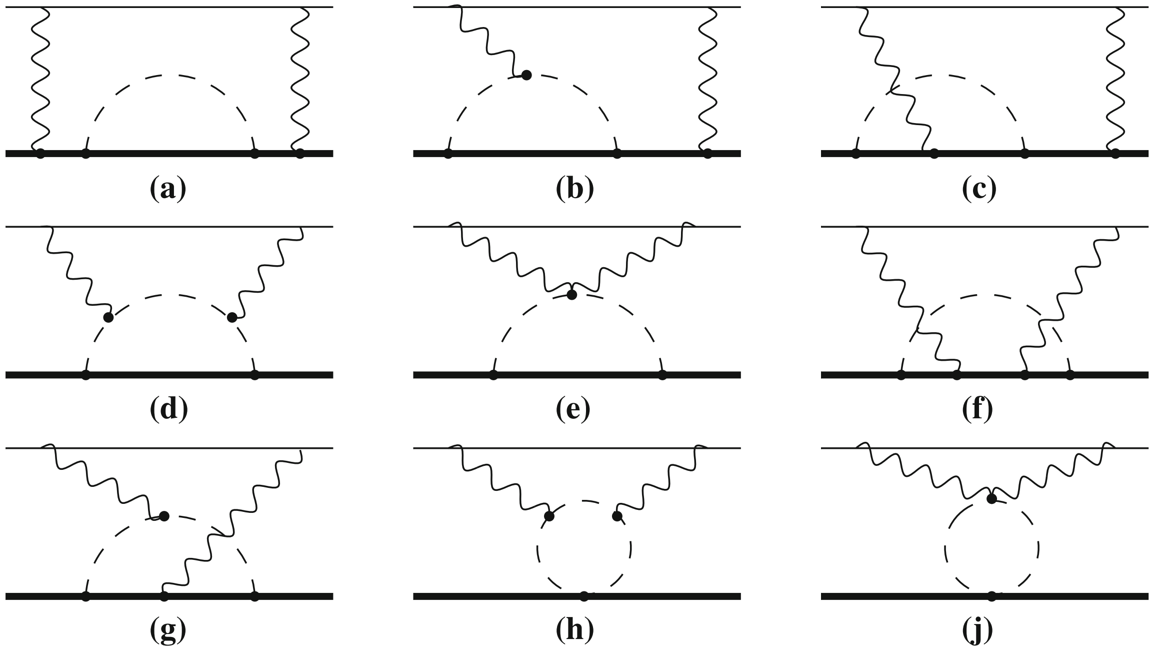

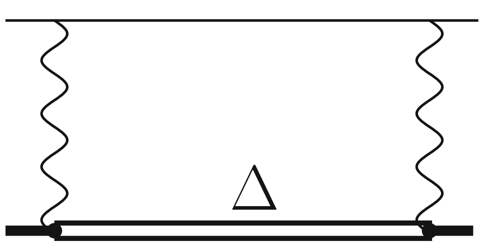

FH, V. Lensky, V. Pascalutsa, EPJC **83** (2023) 8, 762

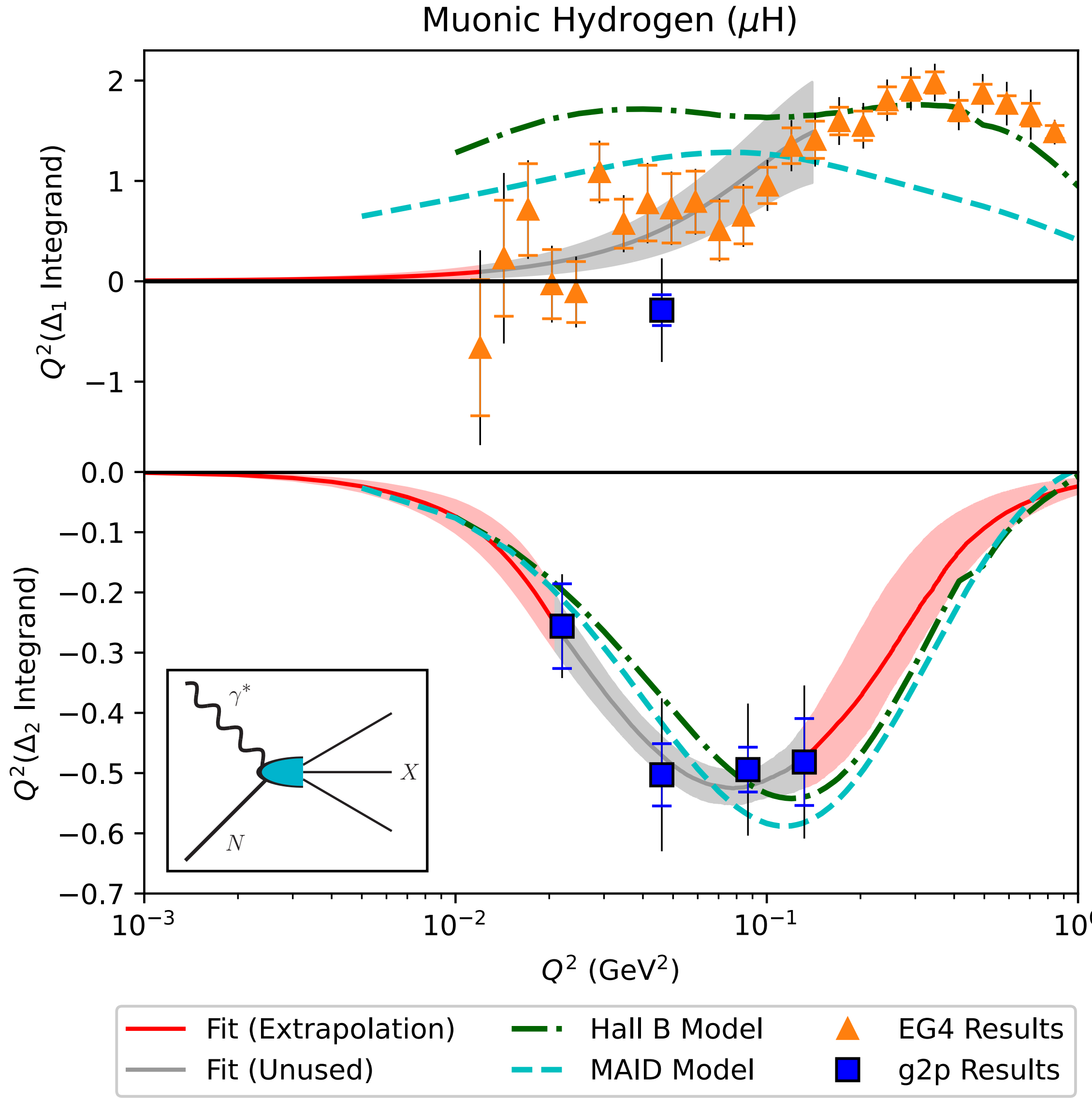

D. Ruth, K. Slifer, J.P. Chen,
C. Carlson, FH, V. Pascalutsa, et al.,
PLB **859** (2024) 139116

Polarizability Effect

BChPT vs. Data-driven Dispersion Relations

Baryon Chiral Perturbation Theory

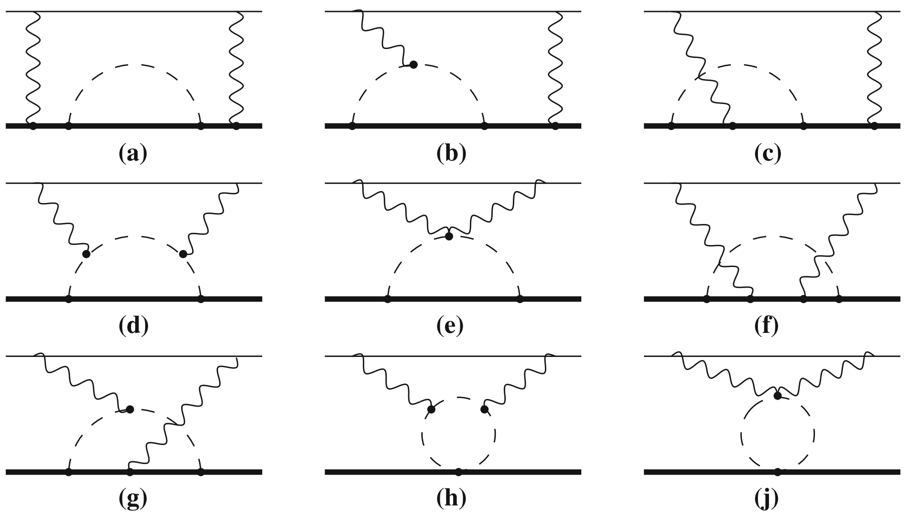

Data-driven dispersive approach

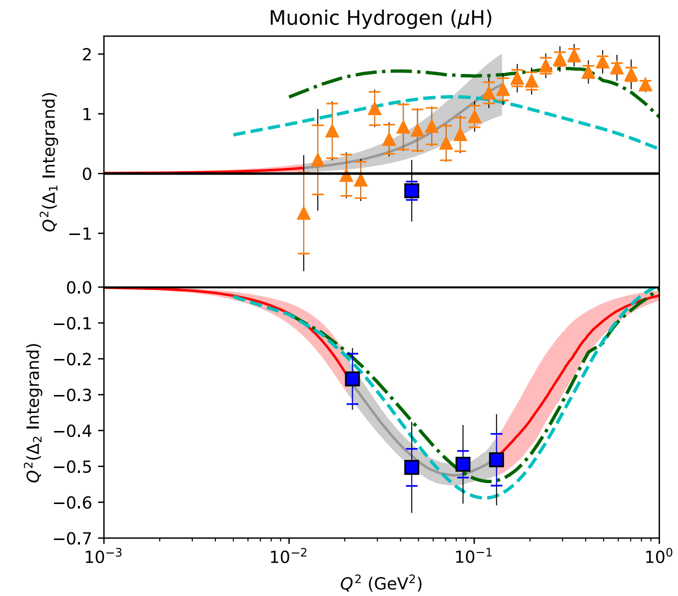

- Spin-dependent forward TPE is completely constrained by empirical information
- TPE effects are dominated by low energies (low photon virtualities Q^2)
  - BChPT = low-energy EFT of QCD

Polarizability Effect

BChPT vs. Data-driven Dispersion Relations

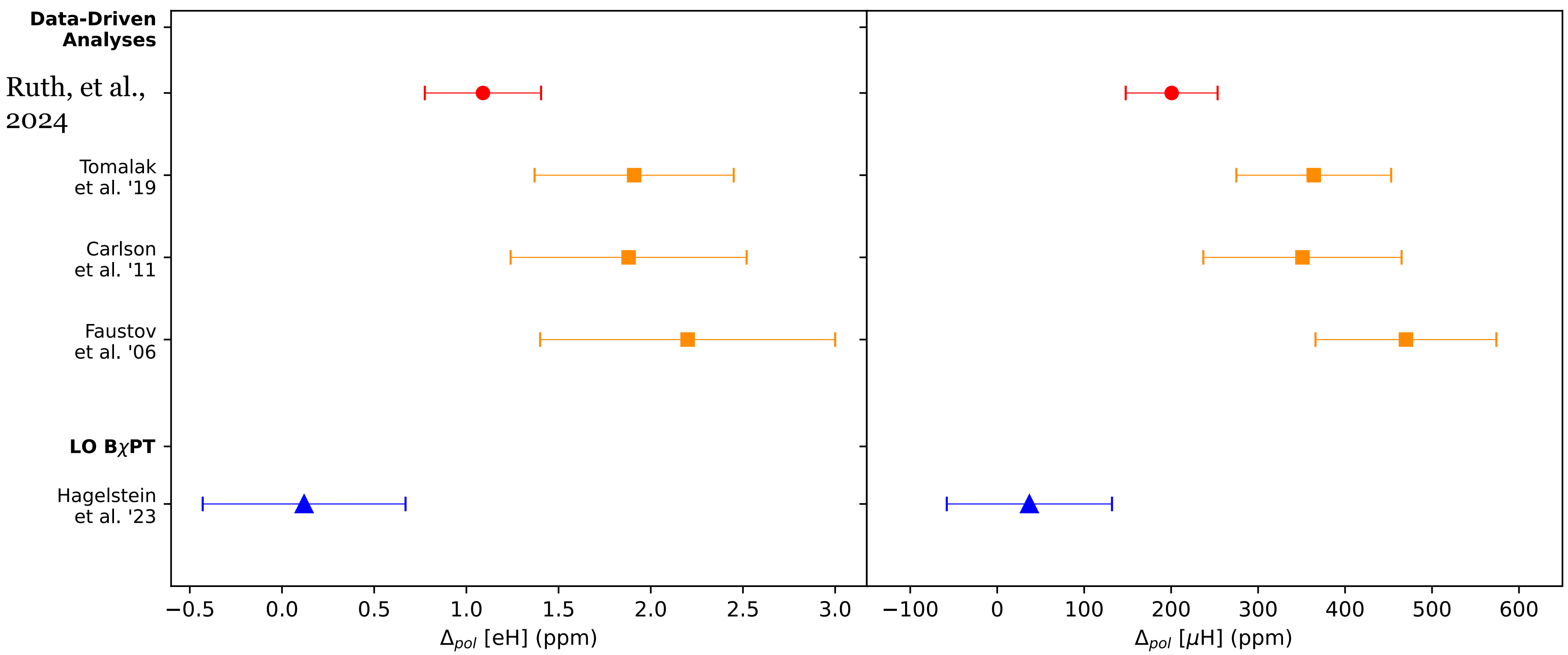

BChPT puts data-driven dispersive evaluation to the test

- Spin-dependent forward TPE is completely constrained by empirical information
- TPE effects are dominated by low energies (low photon virtualities Q^2)
  - BChPT = low-energy EFT of QCD
  - Limited experimental data, e.g., at low Q^2
  - Intricate cancellations enhance uncertainty

Uncertainty Estimate

Partial Integration Trick

Data-driven dispersive approach

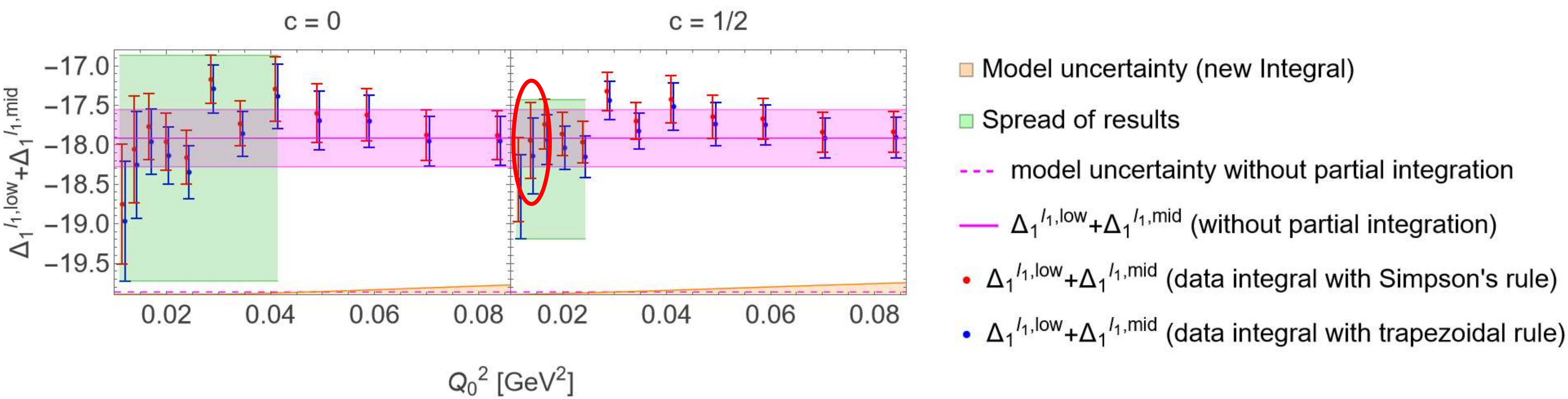

Need to improve understanding at low Q^2

$$\delta_1(\mathrm{H}) \sim \left(\underbrace{-\frac{3}{4}\kappa^2 r_{\mathrm{Pauli}}^2}_{\to -2.19} + \underbrace{18 M^2 c_{1B}}_{\to 3.54} \right) Q_{\mathrm{max}}^2 = 1.35(90),$$

$$\delta_1(\mu\mathrm{H}) \sim \left[\underbrace{-\frac{1}{3}\kappa^2 r_{\mathrm{Pauli}}^2}_{\to -1.45} + \underbrace{8 M^2 c_1}_{\to 2.13} \underbrace{-\frac{M^2}{3\alpha}\gamma_0}_{\to 0.18} \right] \int_0^{Q_{\mathrm{max}}^2} \mathrm{d}Q^2 \beta_1(\tau_\mu) = 0.86(69)$$

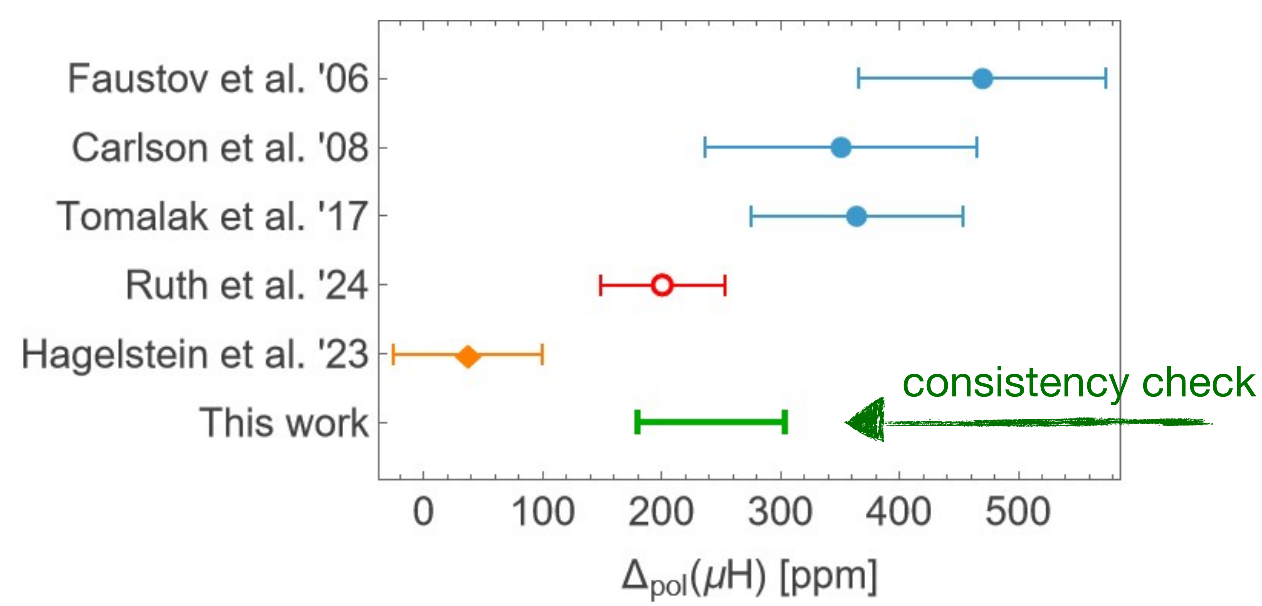

Uncertainty Estimate

$\Delta(1232)$ Contribution

Baryon Chiral Perturbation Theory

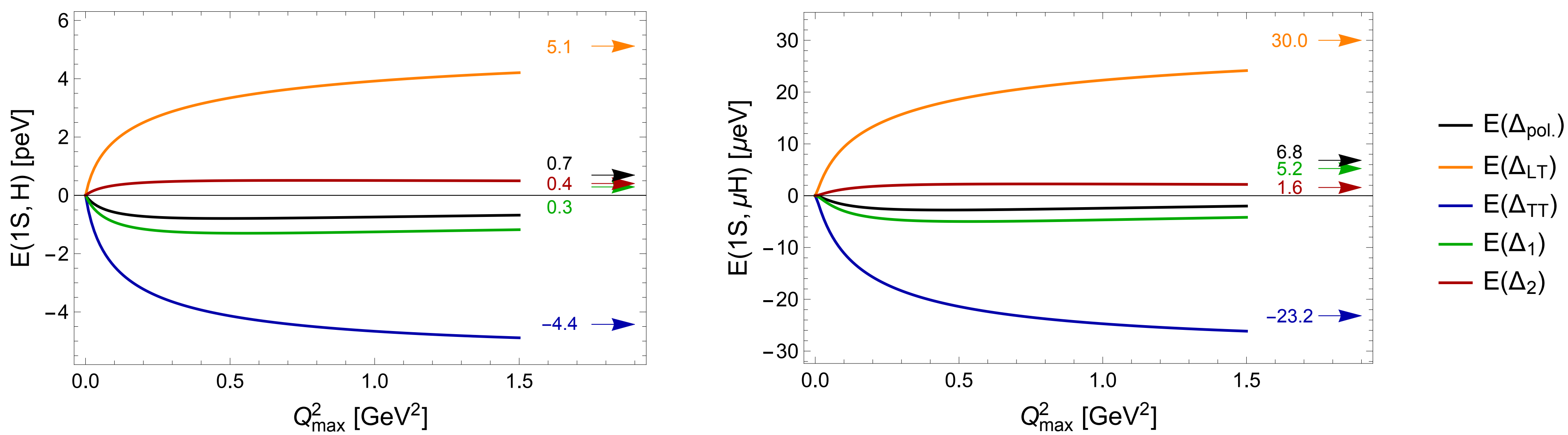

Table 1 Forward 2γ-exchange contribution to the HFS in μH.

Reference	Δ_Z [ppm]	Δ_{recoil} [ppm]	Δ_{pol} [ppm]	Δ_1 [ppm]	Δ_2 [ppm]	$E^{\langle 2\gamma \rangle}_{1S\text{-hfs}}$ [meV]
HEAVY-BARYON χPT						
Peset et al. '17 (13)						−1.161(20)
LEADING-ORDER χPT						
Hagelstein et al. '16 (14)			37(95)	29(90)	9(29)	
$+\Delta(1232)$ EXCIT.						
Hagelstein et al. '18 (15)			−13	84	−97	

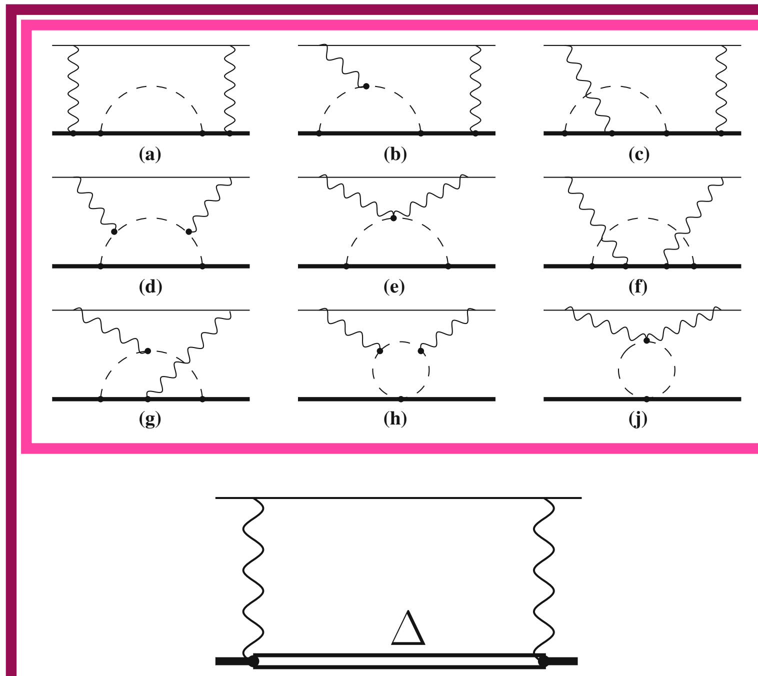

Proton Zemach Radius

From 1S Hyperfine Splitting in H

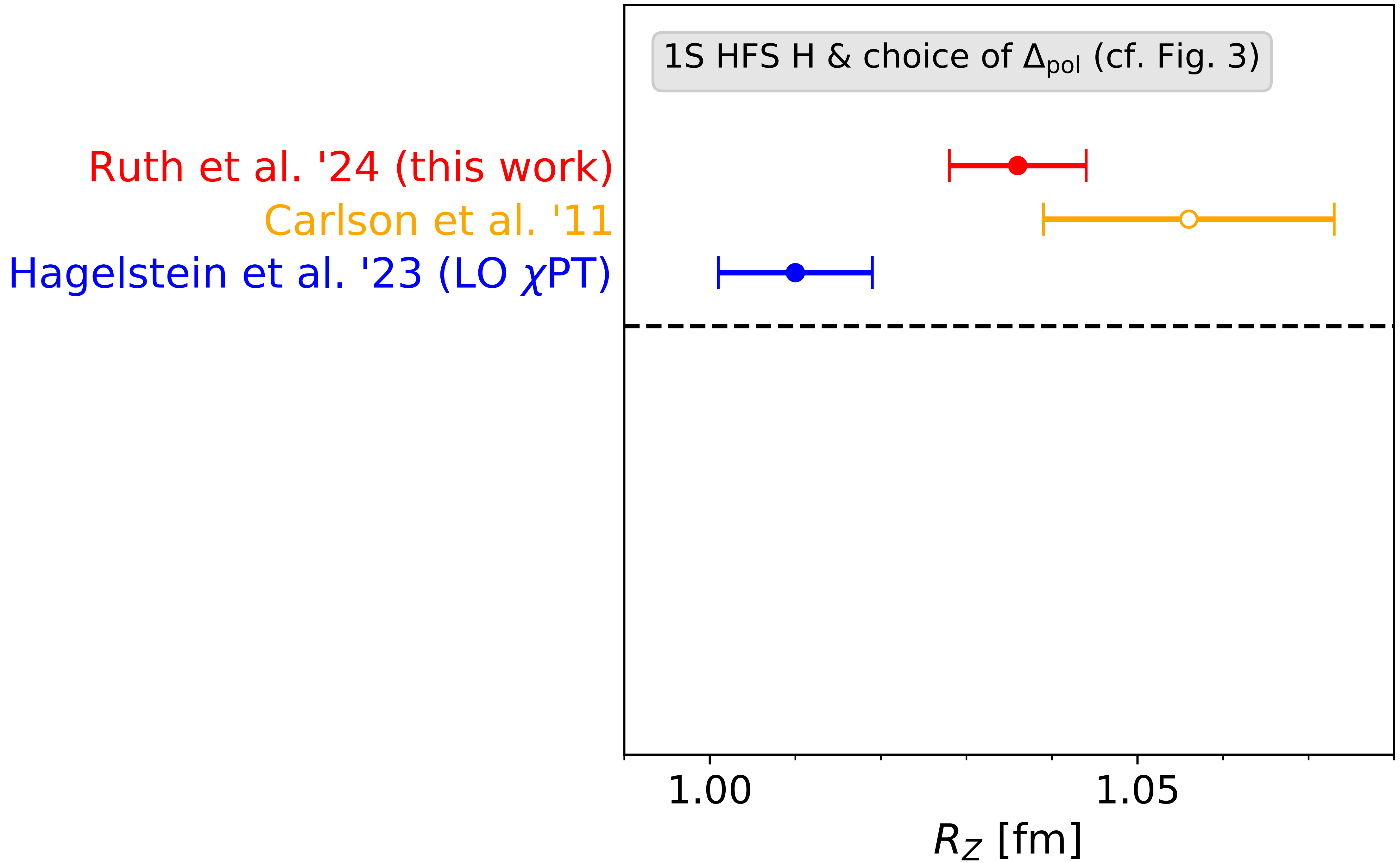

Proton Zemach Radius

From 1S Hyperfine Splitting in H

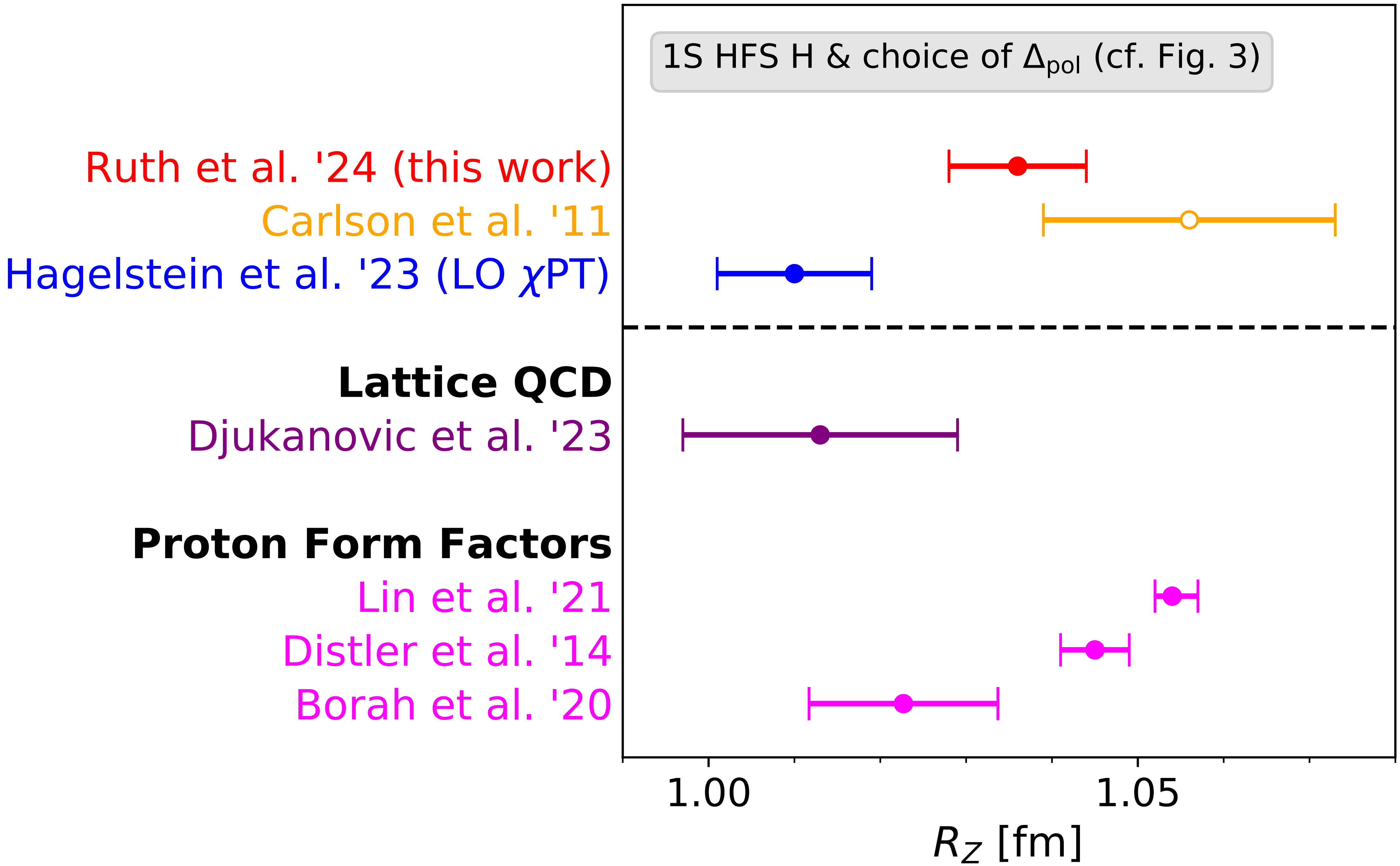

Proton Zemach Radius

Charge Radius Dependence

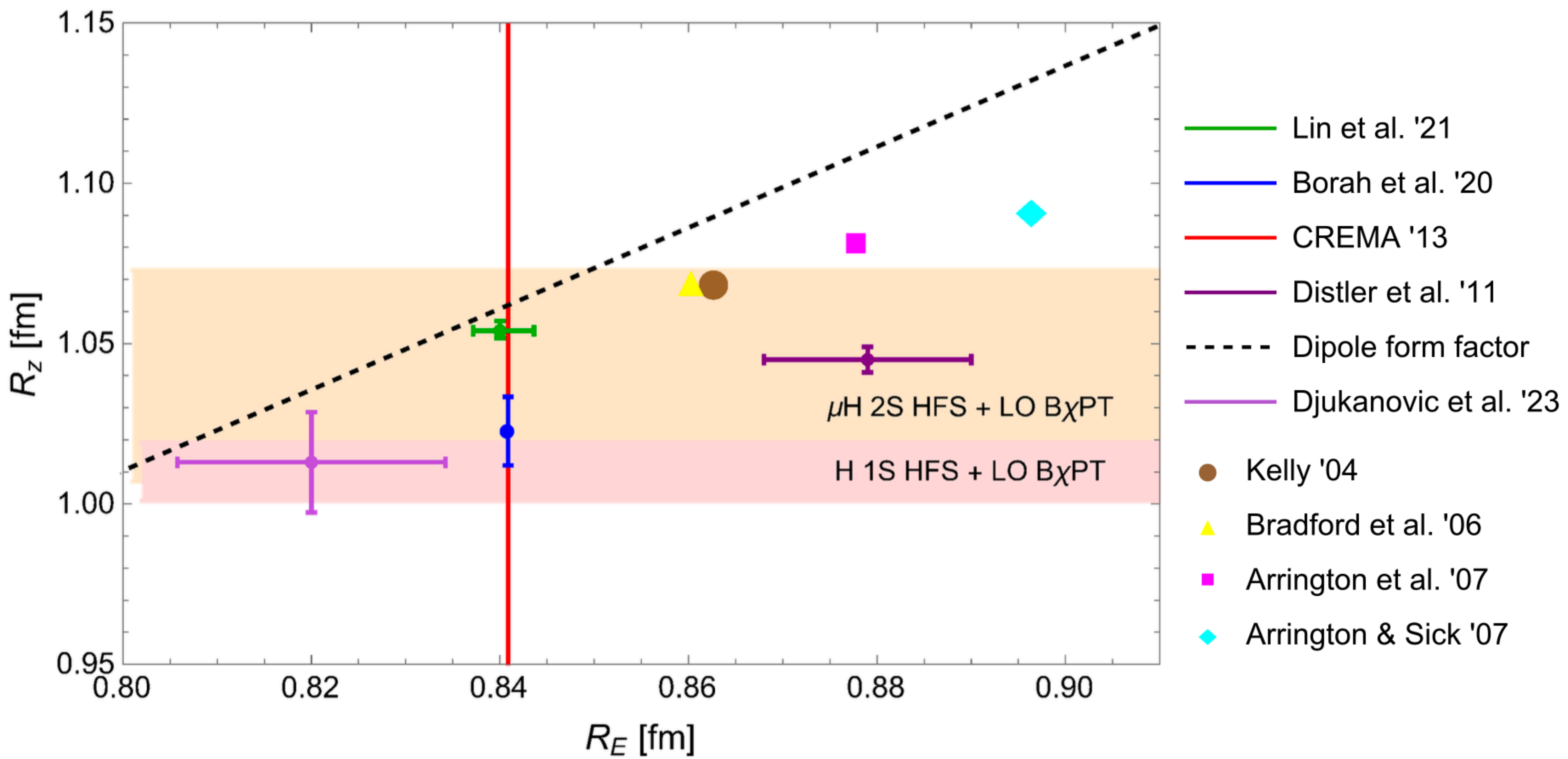

Finite-Size Effects

— Elastic Proton Form Factor Contr. —

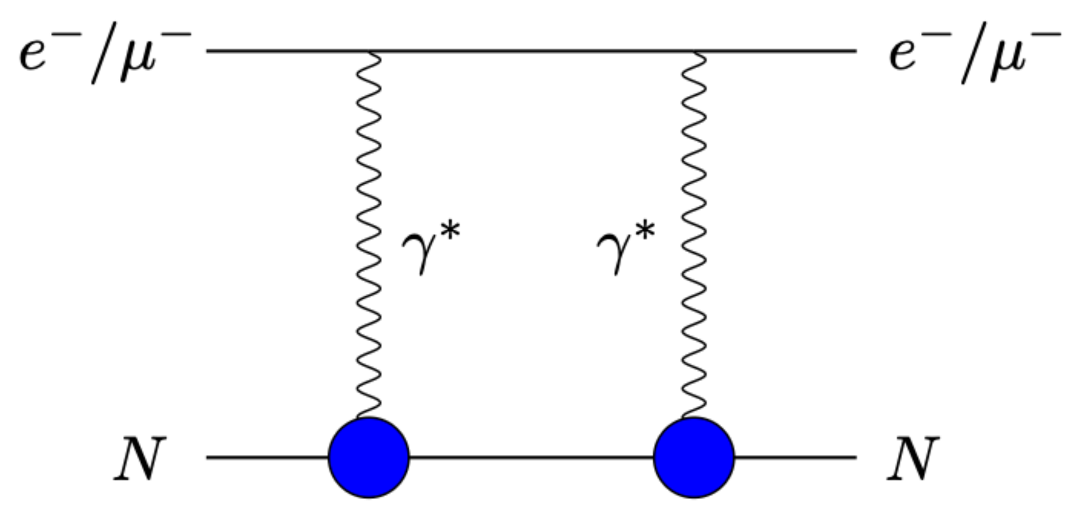

$(Z\alpha)^5$ Recoil Corrections

Form Factor Uncertainties

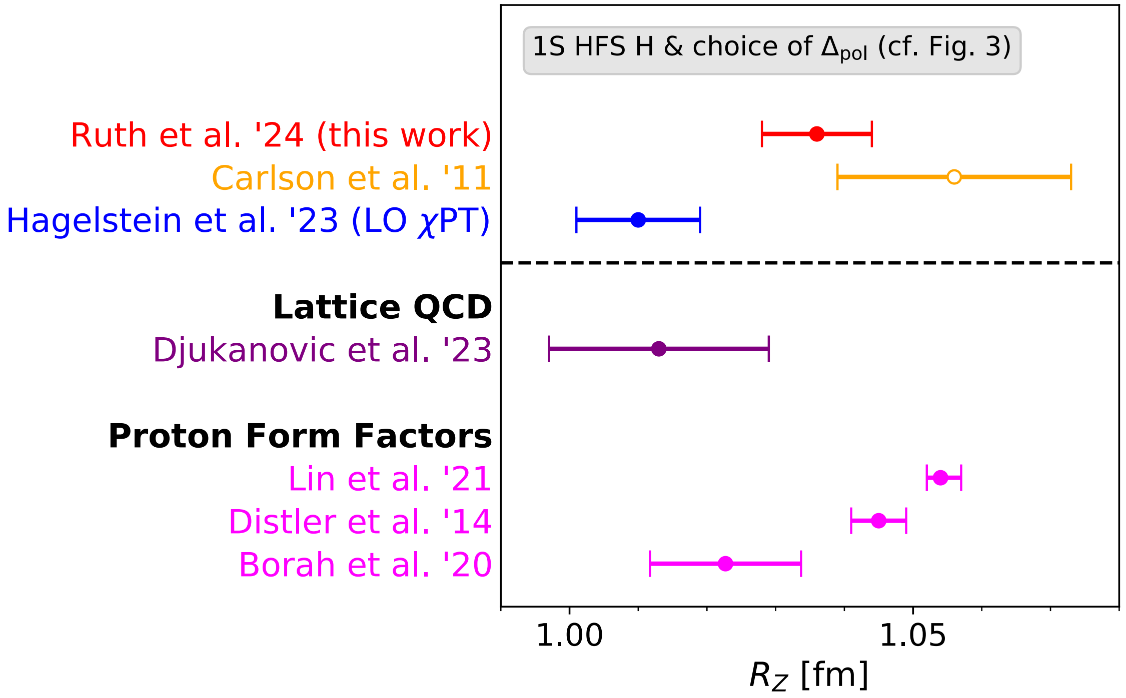

Antognini, Lin, Meißner, PLB **835** (2022) 137575

$$R_Z = 1.054^{+0.003+0.000}_{-0.002-0.001}\ \mathrm{fm}$$

Borah et al., PRD **102** (2020) 7, 074012

$$R_Z = 1.0227(94)(51)\ \mathrm{fm}$$

$(Z\alpha)^5$ Recoil Corrections

Form Factor Uncertainties

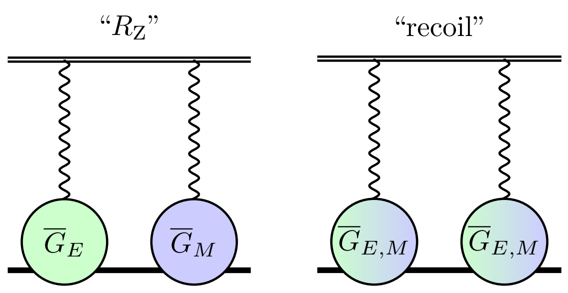

Reference	Δ_Z [ppm]	Δ_{recoil} [ppm]
DATA-DRIVEN		
Carlson et al. '11 (11)[c]	−7703	931
Tomalak '18 (12)[d]	−7333(48)	846(6)
Antognini, Lin, Meißner, PLB **835** (2022) 137575	-7403^{+16}_{-21}	$837.6^{+2.8}_{-1.0}$
Borah et al., PRD **102** (2020) 7, 074012	−7183(75)	849(34)

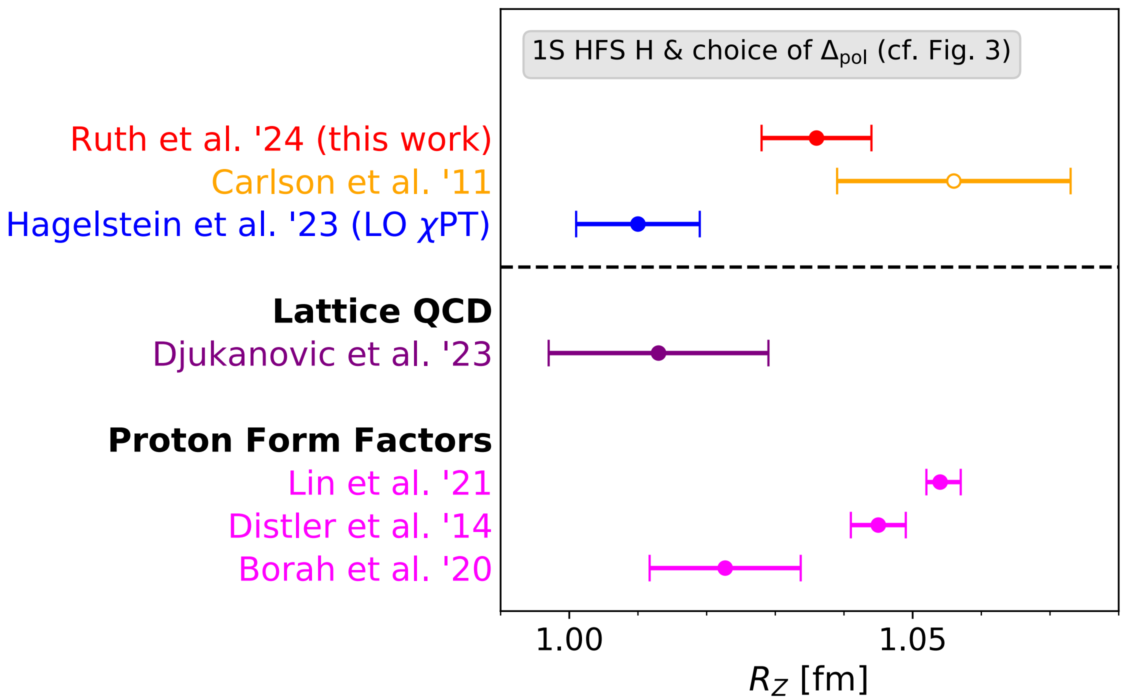

$$R_Z = 1.054^{+0.003+0.000}_{-0.002-0.001}\ \mathrm{fm}$$

$$R_Z = 1.0227(94)(51)\ \mathrm{fm}$$

anticipated experimental precision: 1 - 0.1 ppm

Analysis of Scattering Data

Charge Radius Dependence

- Fitting electron-proton scattering world data:
  - Unpolarized cross sections: 33 experiments, 2055 data points
  - Polarization transfer: 14 experiments, 69 data points
  - Initial-state-radiation extraction: 1 experiment, 25 points
- 10 fixed values of $R_E \in \{0.83, 0.89\}$ fm

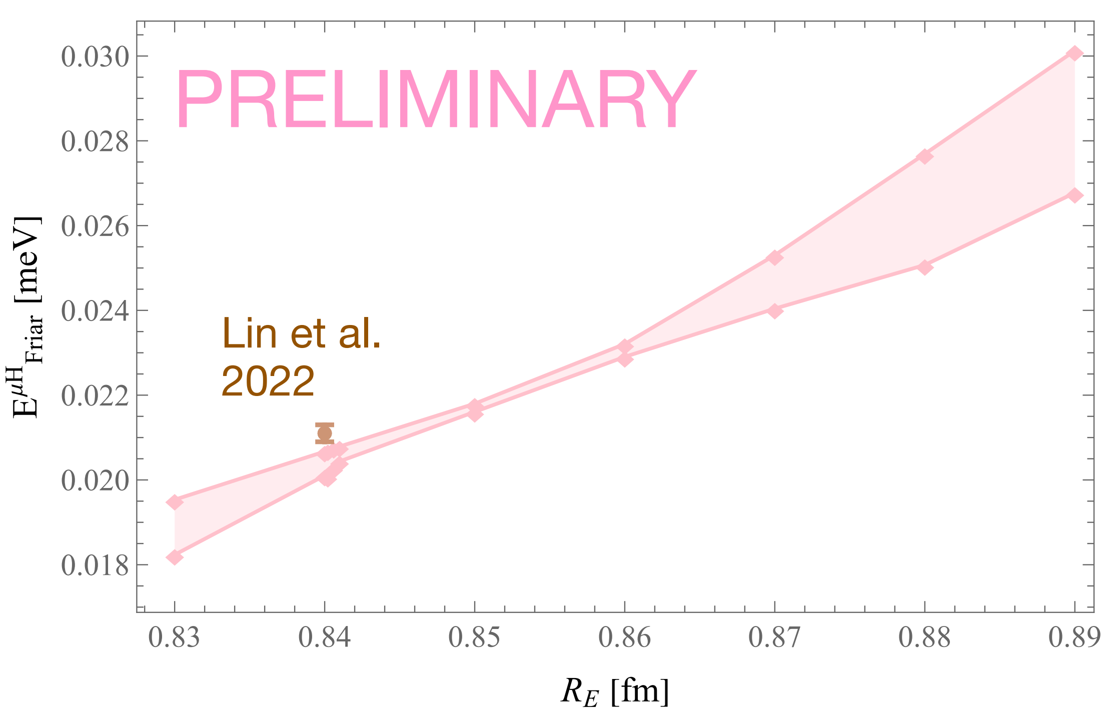

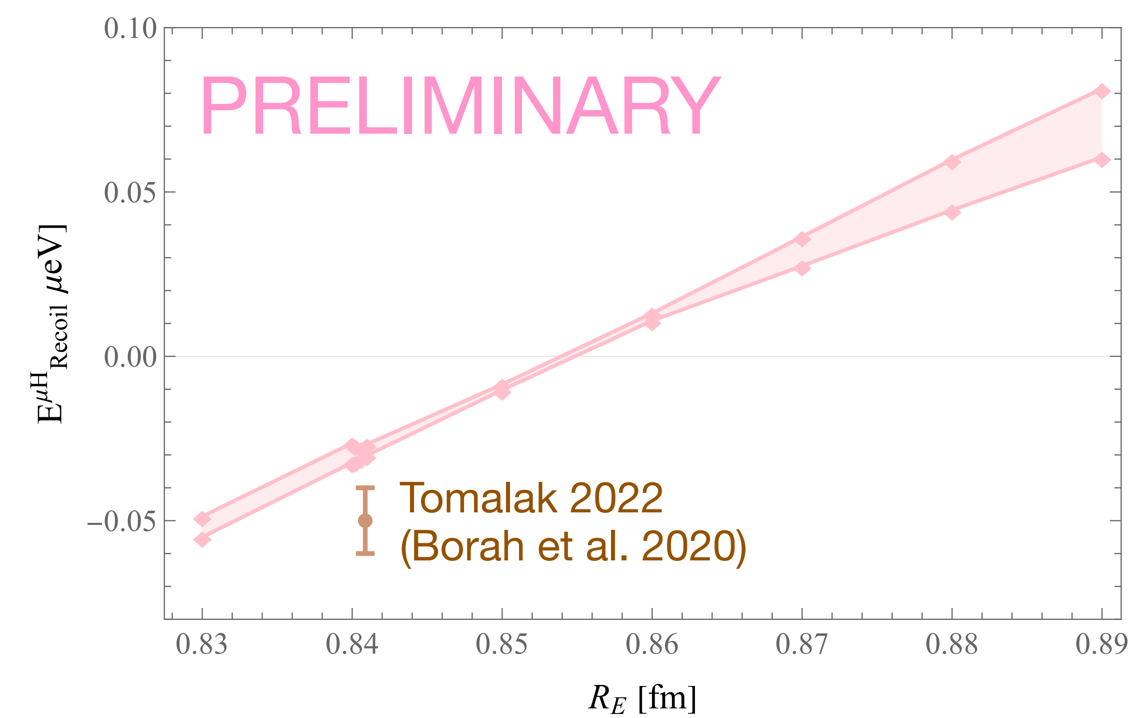

 publication in preparation

Self-Consistent & Blind Extraction

Proton Charge Radius from Lamb Shift

- Experiment: $E_{\mathrm{LS}}^{(\mathrm{exp.})} = 202.370\,6(23)\,\mathrm{meV}$ [CREMA Collaboration (2010/2013)]
- Theory: $E_{\mathrm{LS}}^{(\mathrm{th.})} = \left[206.034\,4(3) - 5.225\,9\,\left(R_E/\mathrm{fm}\right)^2\right]\mathrm{meV} + E_{\mathrm{LS}}^{(\mathrm{strong})}$
  - Our result: $\left[E_{\mathrm{Friar}} + E_{\mathrm{recoil}}\right](R_E)$ + polarizability (BChPT, Pachucki et al. 24)

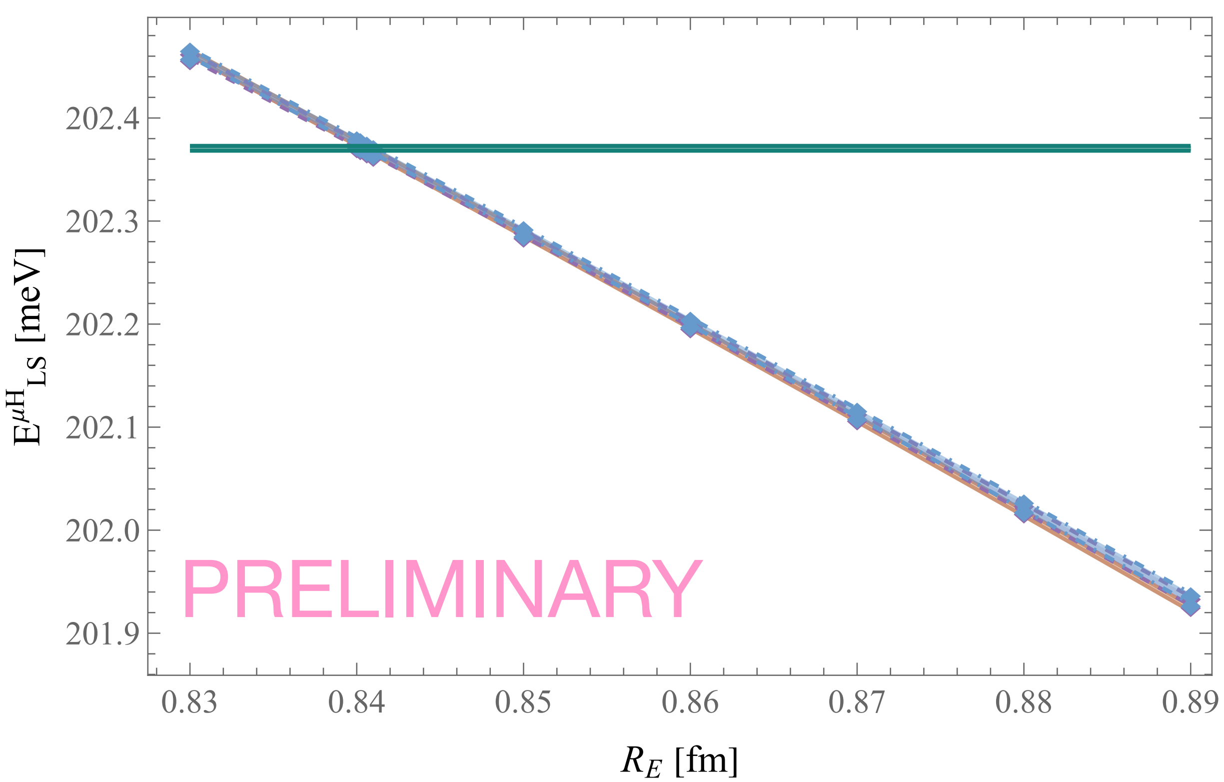

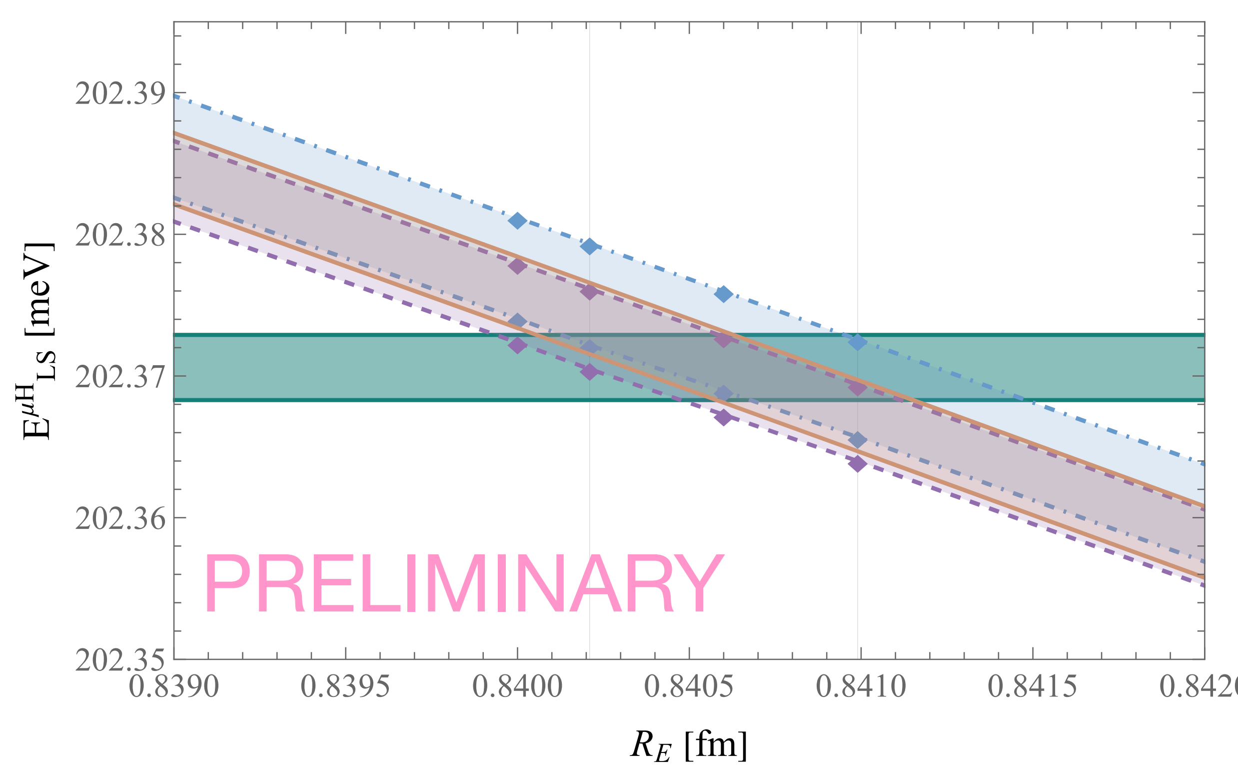

publication in preparation

$(Z\alpha)^6$ Finite-Size Corrections

… Limitation of the $(Z\alpha)^5$ Finite-Size Expansion

		H		μH	
Quantity	Form Factor	Exact [kHz]	$\mathcal{O}(\alpha^5)$ [kHz]	Exact [µeV]	$\mathcal{O}(\alpha^5)$ [µeV]
	Ye et al. [49]	$-38.5(7)$	$-38.5(7)$	$-918(15)$	$-921(15)$
	Borah et al. [50]	$-36.4(5)$	$-36.4(5)$	$-869(13)$	$-871(13)$
$E_{1S-\mathrm{hfs}}$	Exp. Precision	0.000 002		0.02[a]	
	Ye et al. [49]	$-4.82(8)$	$-4.82(8)$	$-114.8(1.9)$	$-115.1(2.0)$
	Borah et al. [50]	$-4.56(7)$	$-4.56(7)$	$-108.7(1.6)$	$-108.9(1.6)$
$E_{2S-\mathrm{hfs}}$	Exp. Precision	0.000 85		5.1	
	Ye et al. [49]	0.000 092(6)		0.404(27)	
	Borah et al. [50]	0.000 069(7)		0.307(33)	
D_{21}	Exp. Precision	0.006 8		40.8[a]	

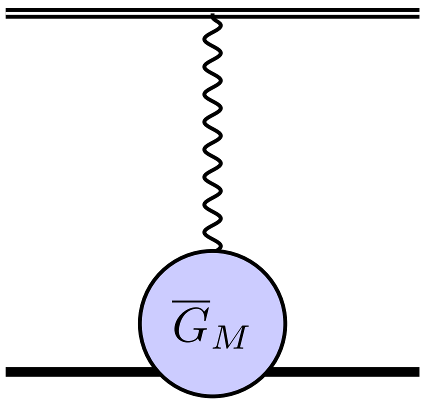

$(Z\alpha)^6$ Finite-Size Corrections

… Limitation of the $(Z\alpha)^5$ Finite-Size Expansion

Quantity	Form Factor	H Exact [kHz]	H $\mathcal{O}(\alpha^5)$ [kHz]	μH Exact [µeV]	μH $\mathcal{O}(\alpha^5)$ [µeV]
$E_{1S-\mathrm{hfs}}$	Ye et al. [49]	−38.5(7)	−38.5(7)	−918(15)	−921(15)
	Borah et al. [50]	−36.4(5)	−36.4(5)	−869(13)	−871(13)
	Exp. Precision	0.000 002		0.02[a]	
$E_{2S-\mathrm{hfs}}$	Ye et al. [49]	−4.82(8)	−4.82(8)	−114.8(1.9)	−115.1(2.0)
	Borah et al. [50]	−4.56(7)	−4.56(7)	−108.7(1.6)	−108.9(1.6)
	Exp. Precision	0.000 85		5.1	
D_{21}	Ye et al. [49]	0.000 092(6)		0.404(27)	
	Borah et al. [50]	0.000 069(7)		0.307(33)	
	Exp. Precision	0.006 8		40.8[a]	

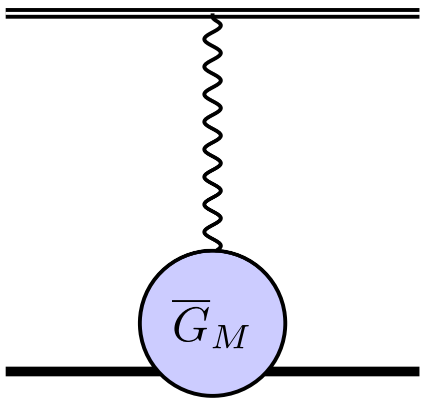

Ye, Arrington, Hill, Lee, PLB 777 (2018) 8–15

$$R_M = 0.851(28)\,\mathrm{fm}$$

Borah et al., PRD **102** (2020) 7, 074012

$$R_M = 0.739(41)\,\mathrm{fm}$$

 publication in preparation

$(Z\alpha)^6$ Finite-Size Corrections

… Limitation of the $(Z\alpha)^5$ Finite-Size Expansion

Quantity	Form Factor	H Exact [kHz]	H $\mathcal{O}(\alpha^5)$ [kHz]	μH Exact [μeV]	μH $\mathcal{O}(\alpha^5)$ [μeV]
$E_{1S-\text{hfs}}$	Ye et al. [49]	$-38.5(7)$	$-38.5(7)$	$-918(15)$	$-921(15)$
	Borah et al. [50]	$-36.4(5)$	$-36.4(5)$	$-869(13)$	$-871(13)$
	Exp. Precision	0.000 002		0.02[a]	
$E_{2S-\text{hfs}}$	Ye et al. [49]	$-4.82(8)$	$-4.82(8)$	$-114.8(1.9)$	$-115.1(2.0)$
	Borah et al. [50]	$-4.56(7)$	$-4.56(7)$	$-108.7(1.6)$	$-108.9(1.6)$
	Exp. Precision	0.000 85		5.1	
D_{21}	Ye et al. [49]	0.000 092(6)		0.404(27)	
	Borah et al. [50]	0.000 069(7)		0.307(33)	
	Exp. Precision	0.006 8		40.8[a]	

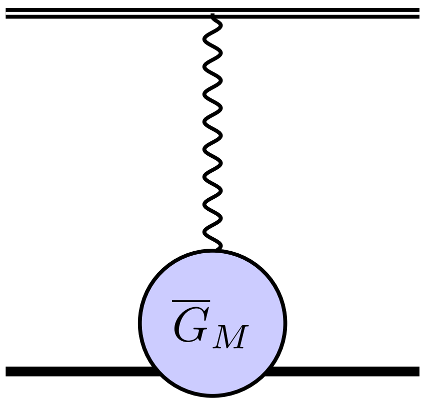

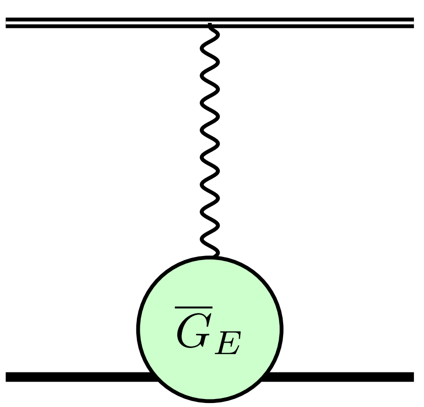

Ye, Arrington, Hill, Lee, PLB 777 (2018) 8–15

$$R_M = 0.851(28)\,\text{fm}$$
$$R_E = 0.879(12)\,\text{fm}$$

Borah et al., PRD **102** (2020) 7, 074012

$$R_M = 0.739(41)\,\text{fm}$$
$$R_E = 0.84089(39)\,\text{fm}$$

publication in preparation

Magnetic Radius Puzzle
Form Factor Uncertainties

Constrain the magnetic radius through inelastic scattering?

$$R_M = \left[\frac{1}{1+2\kappa}\left(-\frac{24 I_2'(0)}{1+\kappa} - \frac{3\kappa}{2M^2} + \langle r^2 \rangle_E\right)\right]^{1/2}$$

Projection assuming 25 %, 15 % and 5 % relative uncertainty for $I_2'(0)$

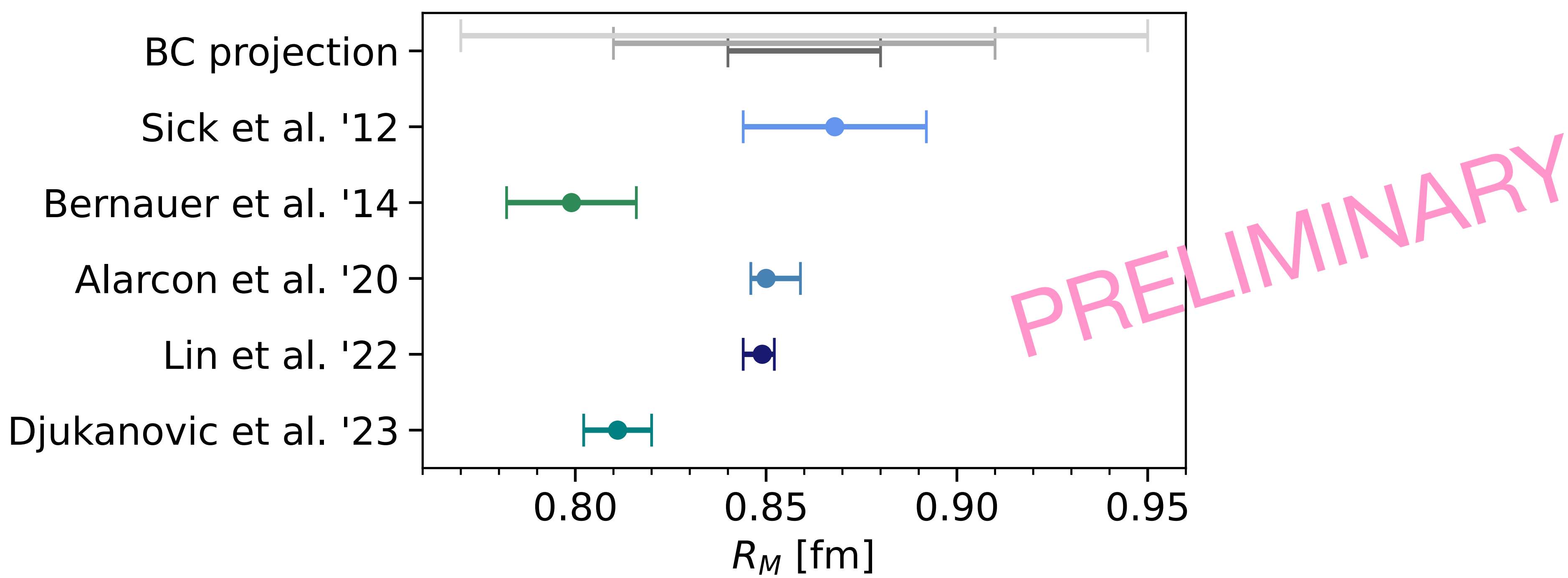

Hadronic Vacuum Polarization

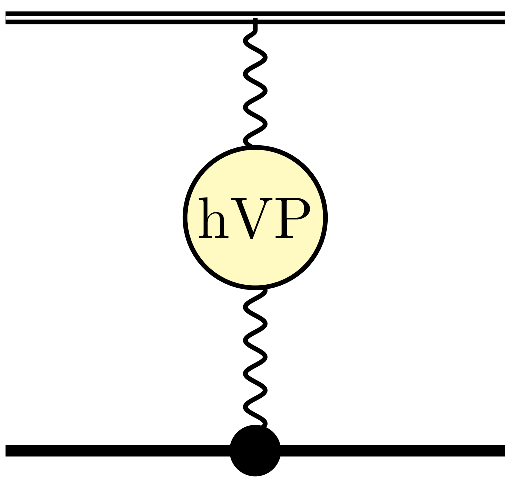

poster by Vadim Lensky

in collaboration with Bogdan Malaescu and Vladimir Pascalutsa

Hadronic Vacuum Polarization

Data-Driven Dispersive Evaluation vs. Lattice QCD

$$\overline{\Pi}(Q^2) = -\frac{Q^2}{\pi}\int \frac{\mathrm{d}t}{t(t+Q^2)}\,\mathrm{Im}\,\Pi(t)$$

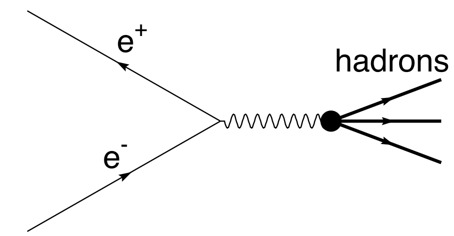

with $\mathrm{Im}\,\Pi(s) = \frac{s}{4\pi\alpha}\sigma(\gamma^* \to \text{anything}) = \frac{\alpha}{3}R(s)$

$$R_\gamma^{\text{had}}(s) = \frac{\sigma(e^+e^- \to \gamma^* \to \text{hadrons})}{\sigma(e^+e^- \to \gamma^* \to \mu^+\mu^-)}$$

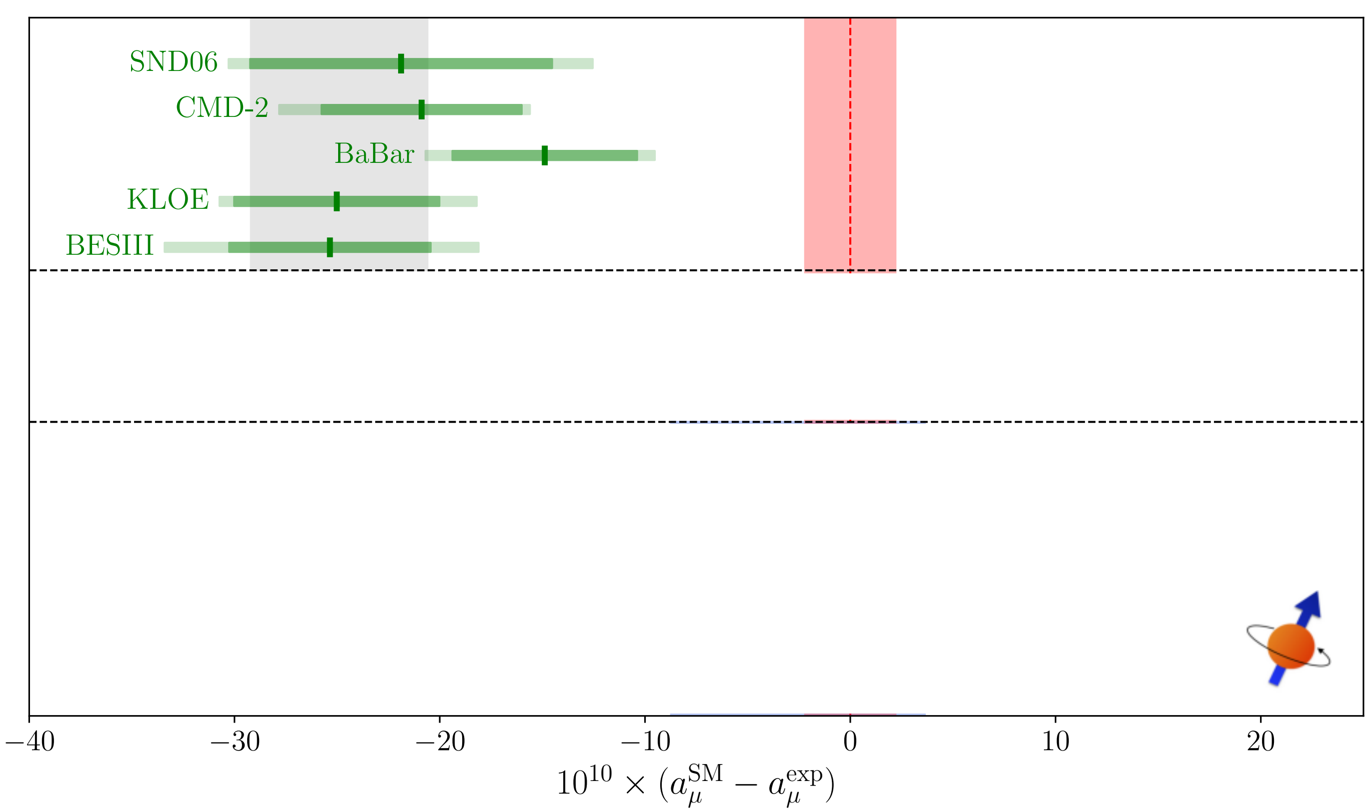

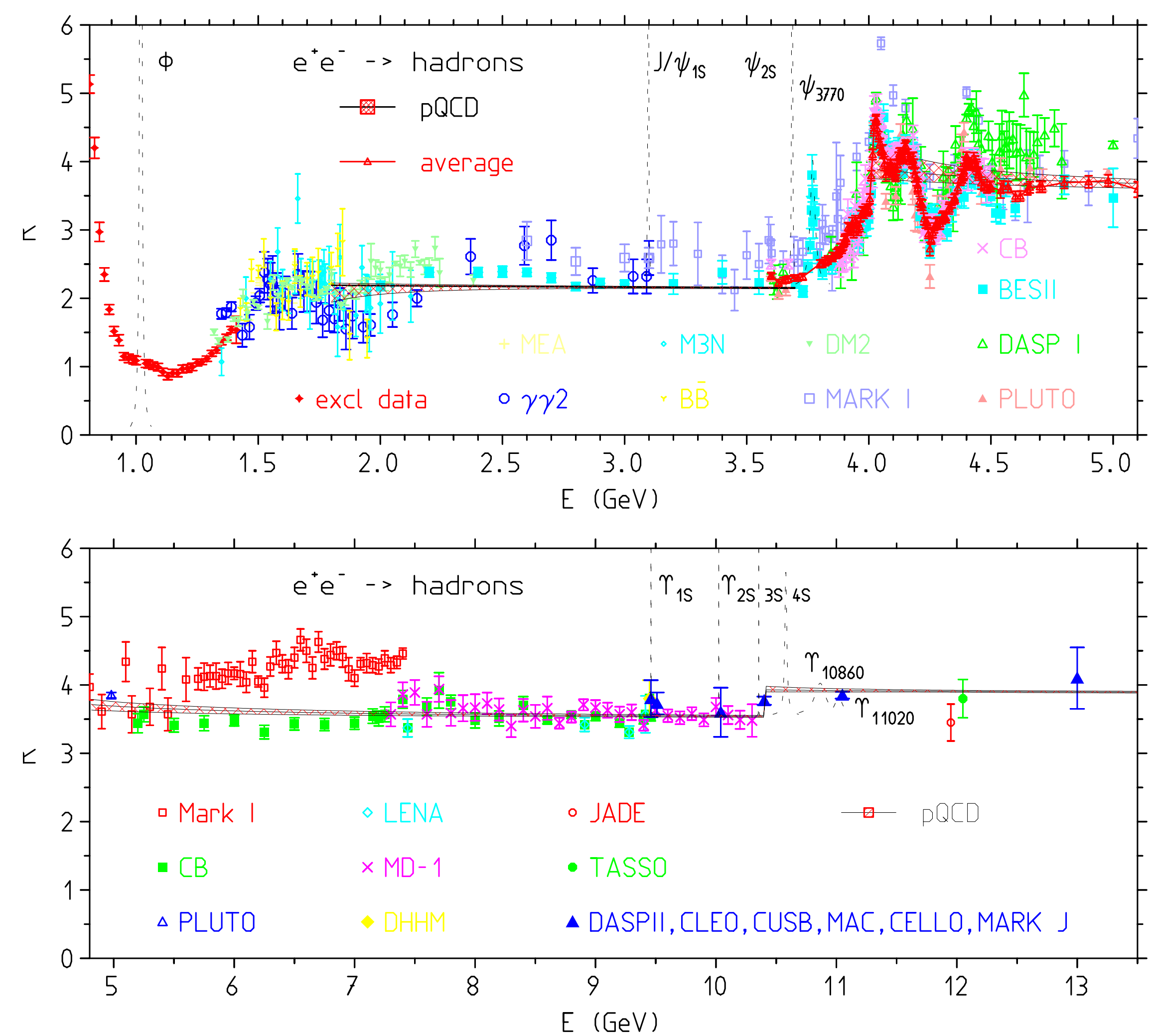

Hadronic Vacuum Polarization

Data-Driven Dispersive Evaluation vs. Lattice QCD

$$\overline{\Pi}(Q^2) = -\frac{Q^2}{\pi}\int \frac{\mathrm{d}t}{t(t+Q^2)}\,\mathrm{Im}\,\Pi(t)$$

with $\mathrm{Im}\,\Pi(s) = \frac{s}{4\pi\alpha}\sigma(\gamma^* \to \text{anything}) = \frac{\alpha}{3}R(s)$

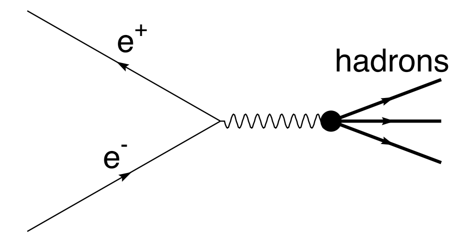

$$R_\gamma^{\text{had}}(s) = \frac{\sigma(e^+e^- \to \gamma^* \to \text{hadrons})}{\sigma(e^+e^- \to \gamma^* \to \mu^+\mu^-)}$$

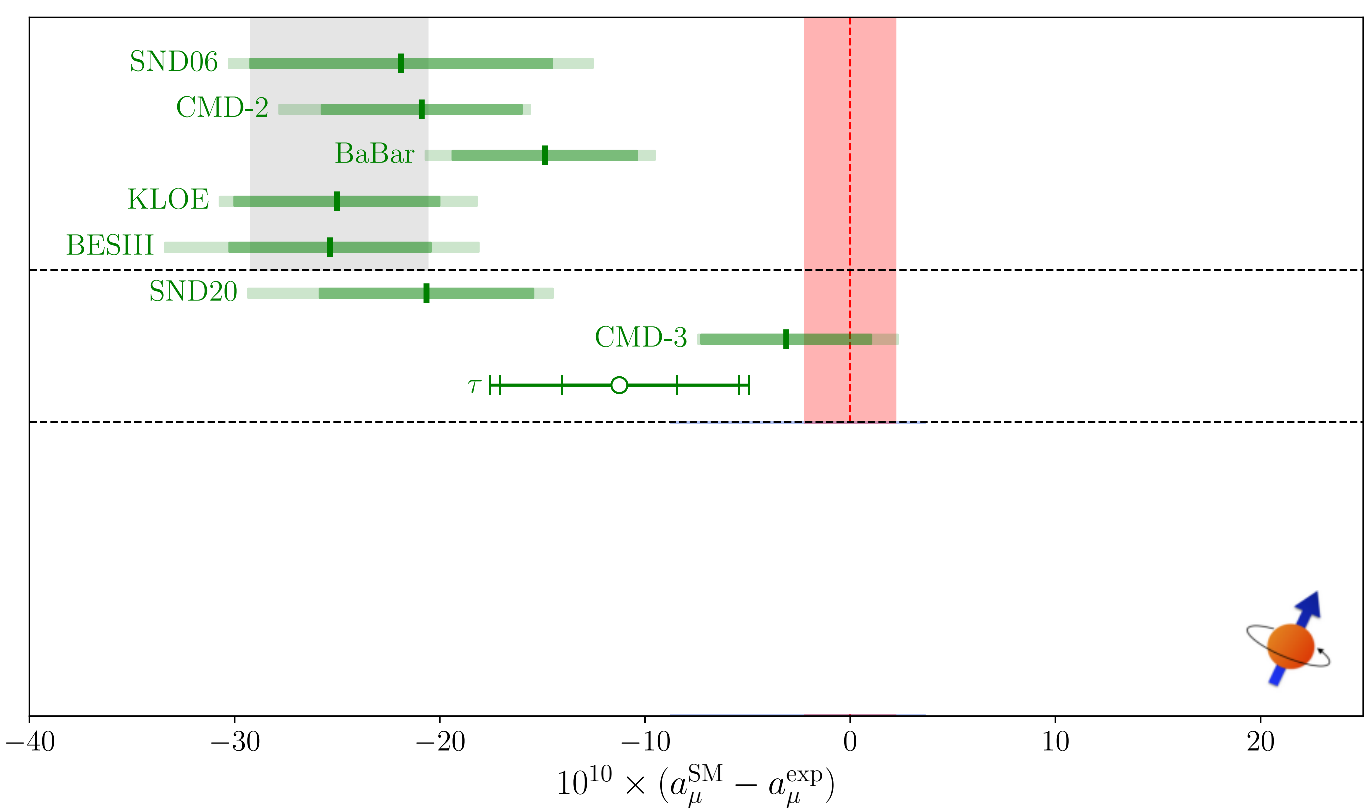

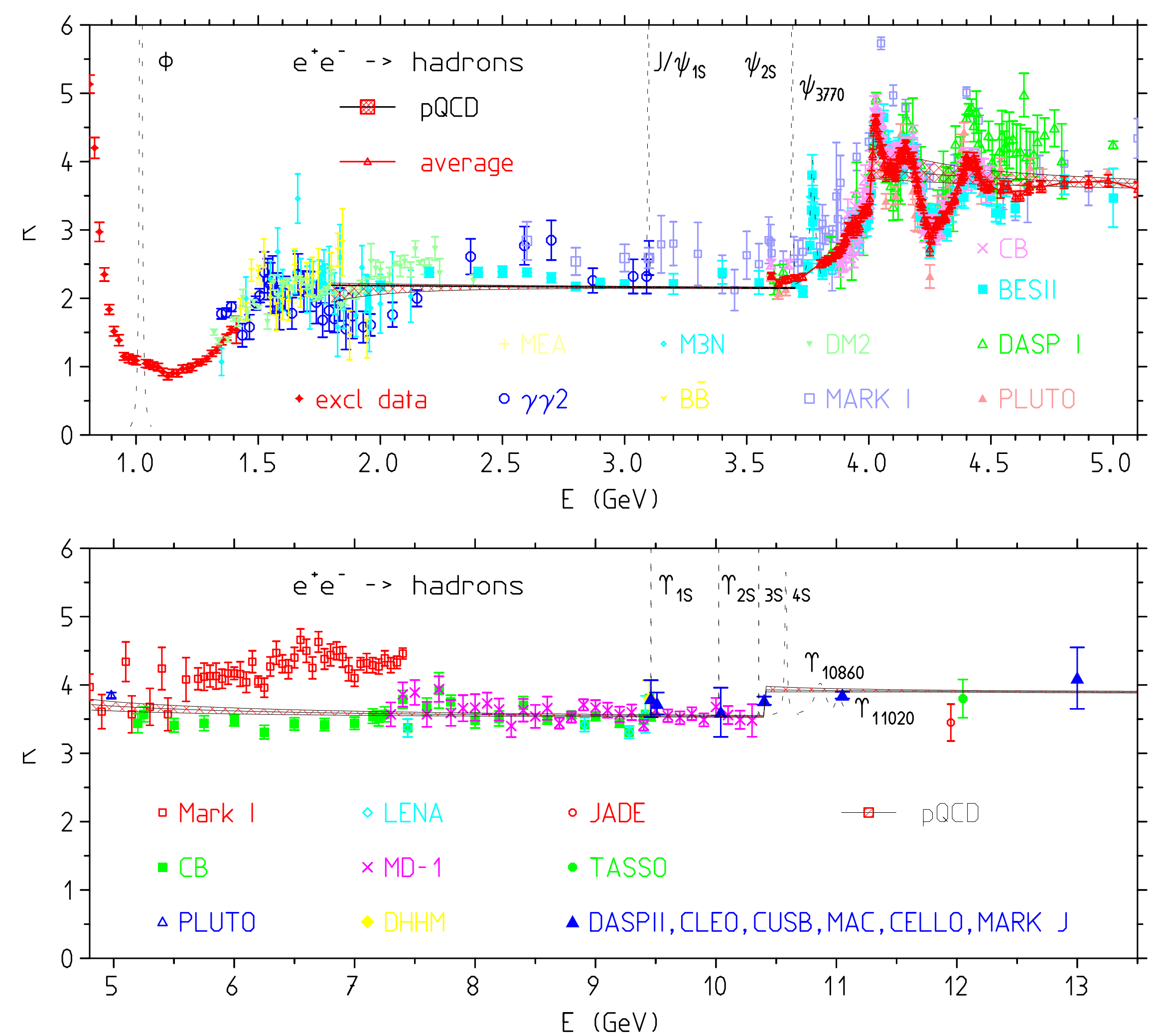

Hadronic Vacuum Polarization

Data-Driven Dispersive Evaluation vs. Lattice QCD

$$\overline{\Pi}(Q^2) = -\frac{Q^2}{\pi}\int \frac{\mathrm{d}t}{t(t+Q^2)}\,\mathrm{Im}\,\Pi(t)$$

with $\mathrm{Im}\,\Pi(s) = \frac{s}{4\pi\alpha}\sigma(\gamma^* \to \text{anything}) = \frac{\alpha}{3}R(s)$

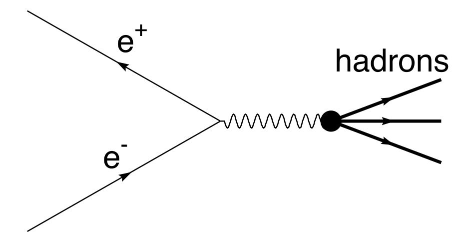

$$R_\gamma^{\text{had}}(s) = \frac{\sigma(e^+e^- \to \gamma^* \to \text{hadrons})}{\sigma(e^+e^- \to \gamma^* \to \mu^+\mu^-)}$$

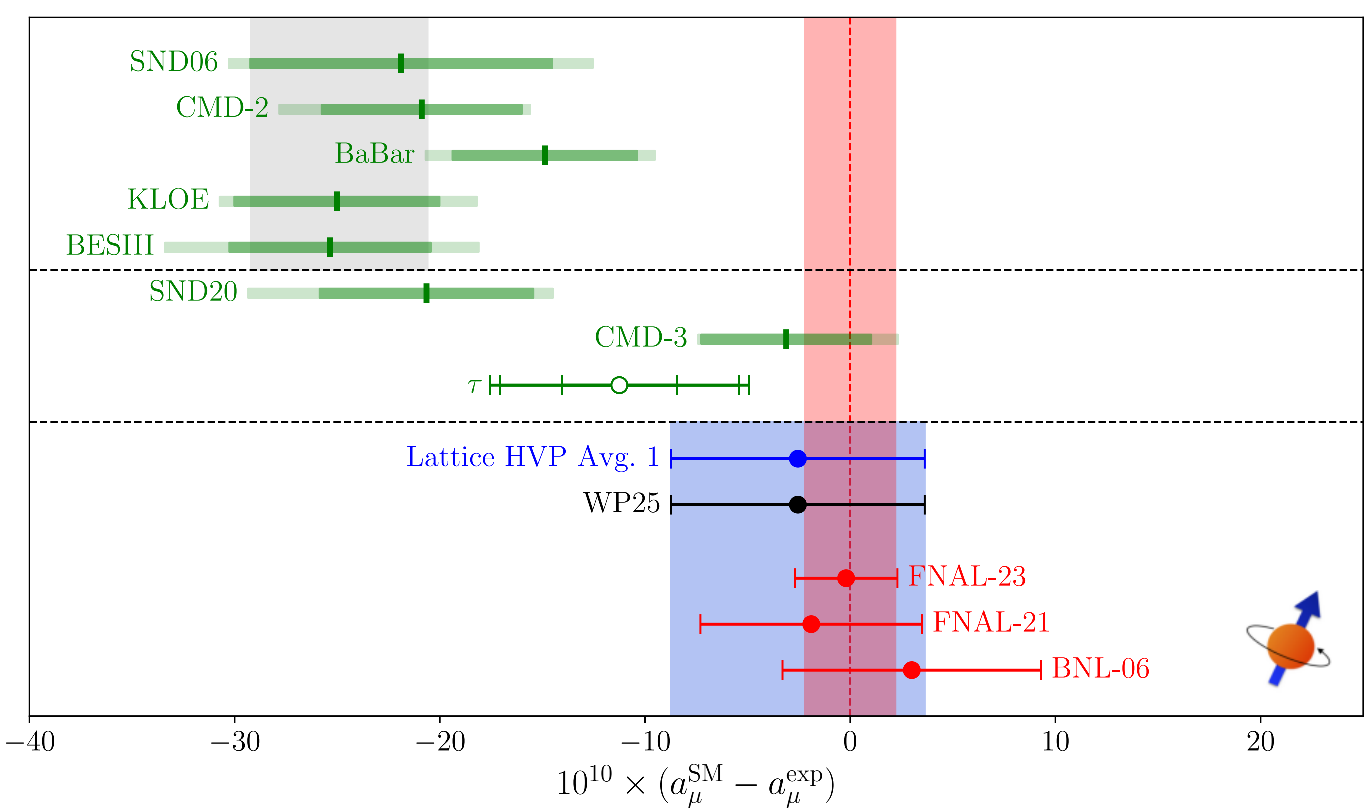

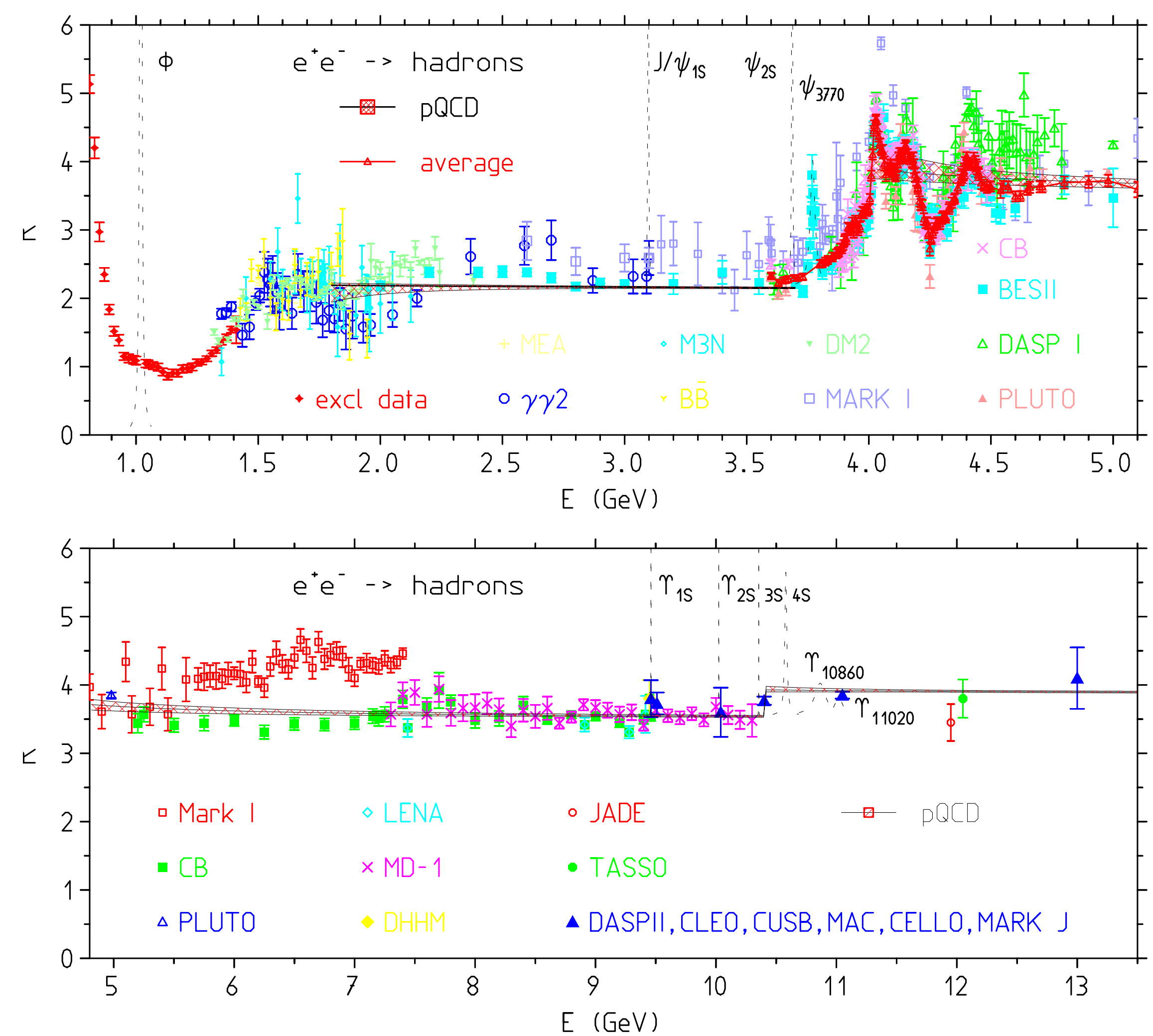

Hadronic Vacuum Polarization

1S Hyperfine Splitting

$$\frac{E^{\mathrm{FS--VP}}_{nS-\mathrm{HFS}}}{E_\mathrm{F}} = -\frac{2Z\alpha}{\pi^2 n^3}\frac{mM}{M^2-m^2}\int_{t_0}^{\infty}\mathrm{d}t\,\frac{\mathrm{Im}\Pi(-t)W(t)}{t}$$

$$= \frac{2Z}{n^3}\left(\frac{\alpha}{\pi}\right)^2\frac{mM}{M^2-m^2}\int_{t_0}^{\infty}\mathrm{d}t\,\frac{R(t)W(t)}{3t}$$

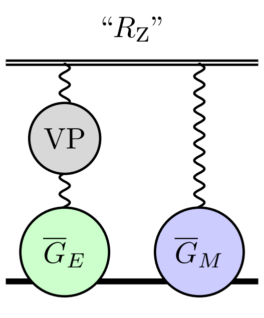

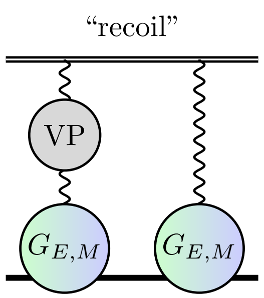

$$W(t) = \frac{1}{1+\kappa}\int_0^\infty \frac{\mathrm{d}Q}{Q}\left\{2(\nu-\nu_l)G_M(Q^2)\left[2F_1(Q^2)+\frac{F_1(Q^2)+3F_2(Q^2)}{(\nu_l+1)(\nu+1)}\right]-\left[1-\frac{m^2}{M^2}\right]\frac{5+4\nu_l}{(1+\nu_l)^2}F_2^2(Q^2)\right\}\frac{Q^2}{t+Q^2}$$

	H [kHz]	^{3}He$^+$ [kHz]	μH [μeV]	μ^3He$^+$ [μeV]
Previous calculations:				
S. Karshenboim, Phys. Lett. A **225**, 97 (1997)				
point-like	0.19(8)			
finite size	0.04(1)			
R. Faustov, A. Martynenko, Phys. Atom. Nucl. **61**, 471 (1998)			3.561 0	
E. Borie, Ann. Phys. **327**, 733 (2012)			4.8(8)	−72.8
This work:				
`DHMZ`	0.086 0(4)	−0.476(17)	2.152(10)	−15.18(55)
`alphaQED23`	0.086 0(5)	−0.476(17)	2.153(14)	−15.17(55)

expect $\times 2$ uncertainty increase due to scatter

soon on arxiv :)

(Muonic) Vacuum Polarization

1S Hyperfine Splitting

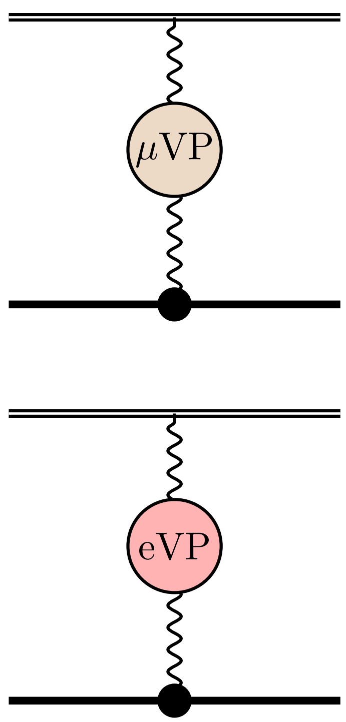

μVP non-recoil (×100)

μVP recoil (×100)

eVP non-recoil

eVP recoil

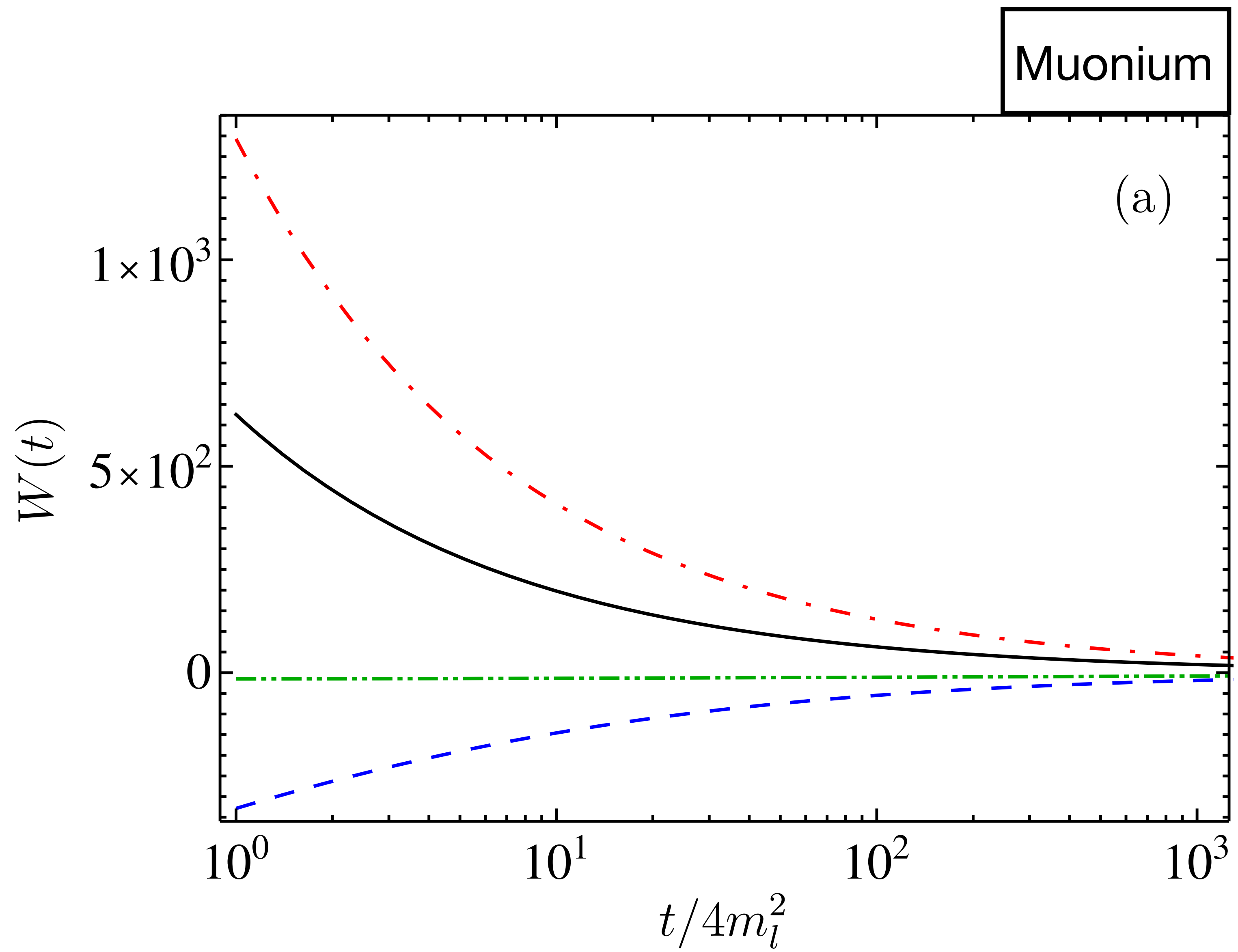

Hadronic Vacuum Polarization

1S Hyperfine Splitting

	Mu [kHz]	H [kHz]	$^3He^+$ [kHz]	μH [μeV]	μ^3He^+ [μeV]
ALPHAQED23					
finite size					
full kernel (12)		0.086 0(5)	−0.476(17)	2.153(14)	−15.17(55)
non-recoil (13)		0.087 6(6)	−0.482(18)	2.093(13)	−15.22(56)
point-like					
full kernel (14)		0.274 5(19)	−2.264(15)	7.07(5)	−73.99(49)
non-recoil (17)		0.397(3)	−4.85(3)	9.49(7)	−152.9(11)
structureless					
full kernel (15)	0.233 8(15)	0.212 8(14)	−3.45(2)	5.51(4)	−112.0(8)

$G_E(Q^2) = 1$,
$G_M(Q^2) = 1 + \kappa$

$\kappa = 0$

Muonic Hydrogen

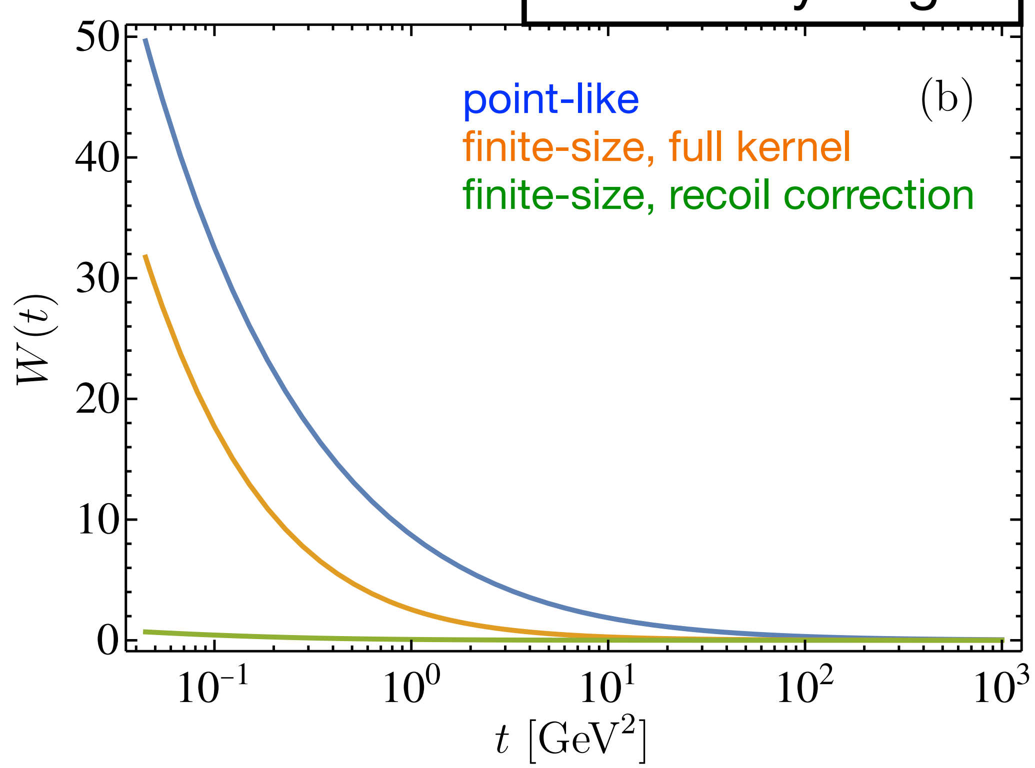

Hadronic Vacuum Polarization

1S Hyperfine Splitting

	Mu [kHz]	H [kHz]	^{3}He$^+$ [kHz]	μH [μeV]	μ^3He$^+$ [μeV]
ALPHAQED23					
finite size					
full kernel (12)		0.086 0(5)	−0.476(17)	2.153(14)	−15.17(55)
non-recoil (13)		0.087 6(6)	−0.482(18)	2.093(13)	−15.22(56)
point-like					
full kernel (14)		0.274 5(19)	−2.264(15)	7.07(5)	−73.99(49)
non-recoil (17)		0.397(3)	−4.85(3)	9.49(7)	−152.9(11)
structureless					
full kernel (15)	0.233 8(15)	0.212 8(14)	−3.45(2)	5.51(4)	−112.0(8)
πVP [13]					
finite size					
full kernel (12)		0.062 4	−0.353(6)	1.561	−11.27(20)
non-recoil (13)		0.063 5	−0.358(6)	1.519	−11.31(20)
point-like					
full kernel (14)		0.168 5	−1.29	4.315	−42.46
non-recoil (17)		0.203 1	−2.48	4.855	−78.23
structureless					
full kernel (15)	0.161 5	0.134 1	−2.04	3.454	−66.15

πVP model by Biloshytskyi et al., 2509.08115

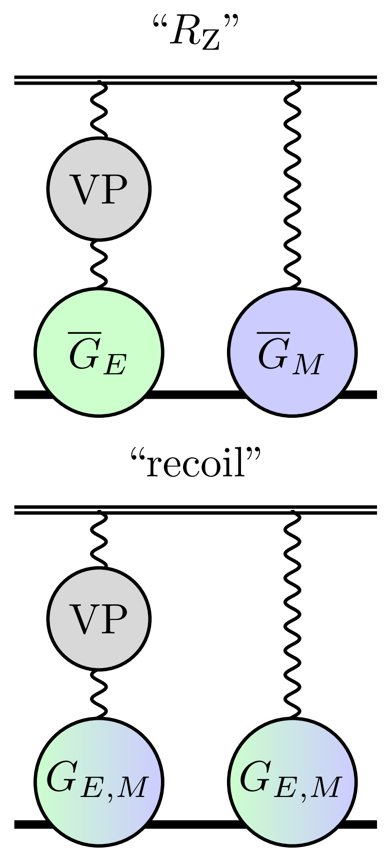

Summary & Conclusions

hadronic = HVP + Zemach radius + finite-size recoil + polarizability

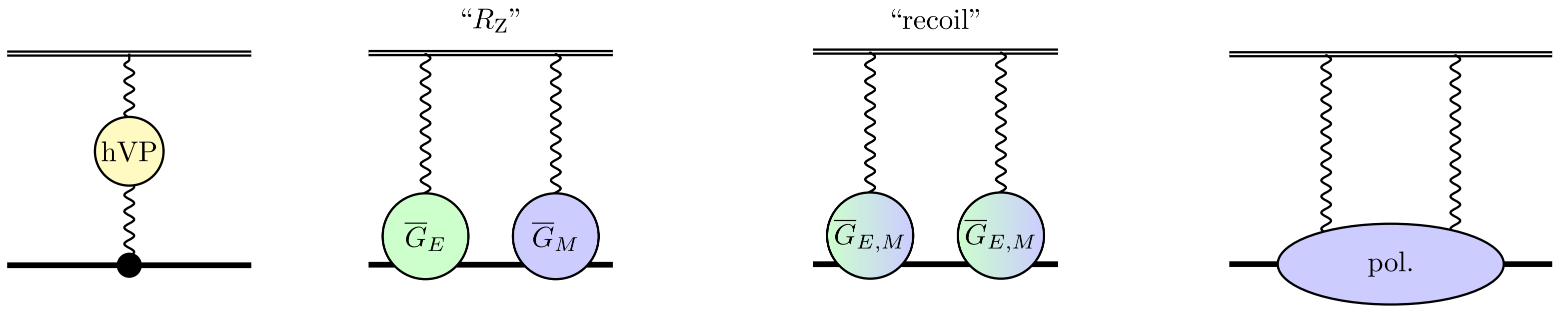

Summary & Conclusions

hadronic = HVP + Zemach radius + finite-size recoil + polarizability

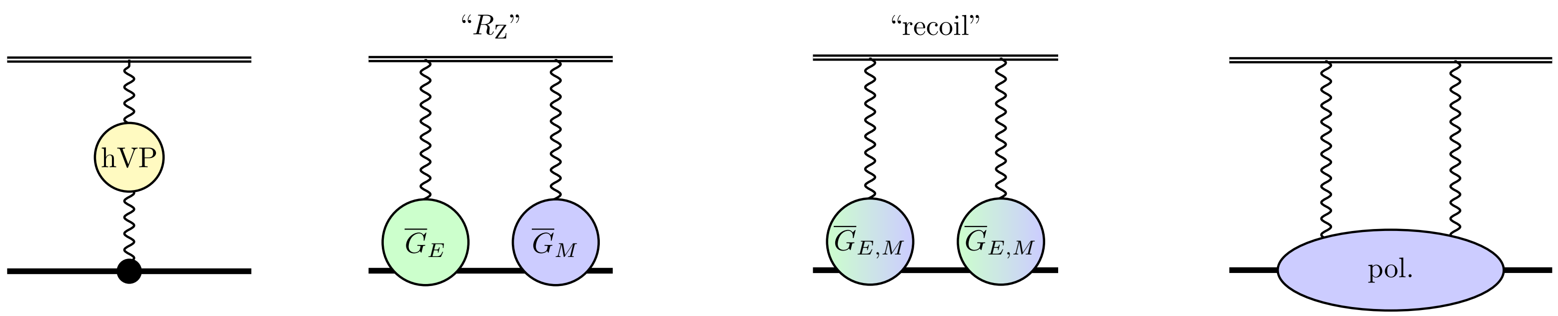

- **Proton-polarizability contribution:**
  - Small discrepancy between BChPT and data-driven predictions remains

Summary & Conclusions

hadronic = HVP + Zemach radius + finite-size recoil + polarizability

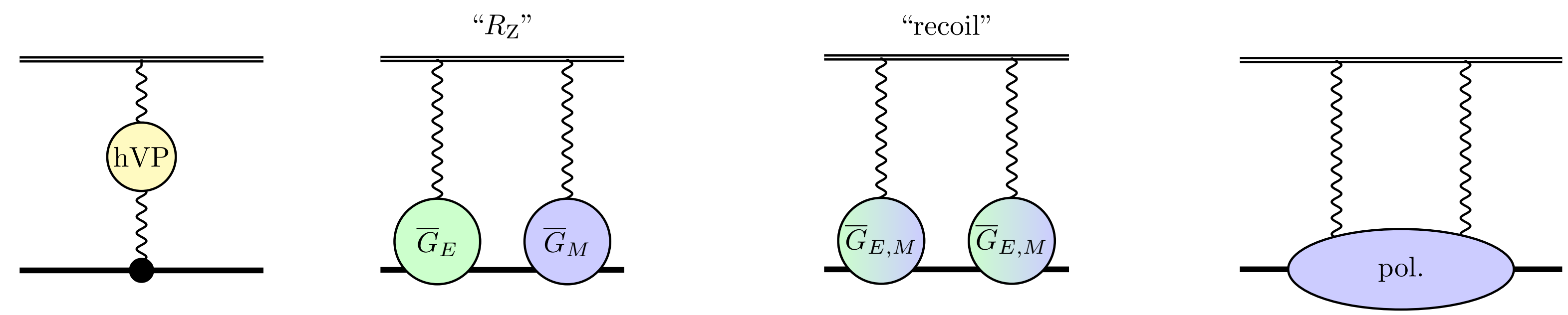

- **Proton-polarizability contribution:**
  - Small discrepancy between BChPT and data-driven predictions remains
- **Finite-size (Zemach radius and recoil) corrections:**
  - Require careful assessment of model uncertainties in form factor input
  - Self-consistent radii extractions from scattering and spectroscopy desired

Summary & Conclusions

hadronic = HVP + Zemach radius + finite-size recoil + polarizability

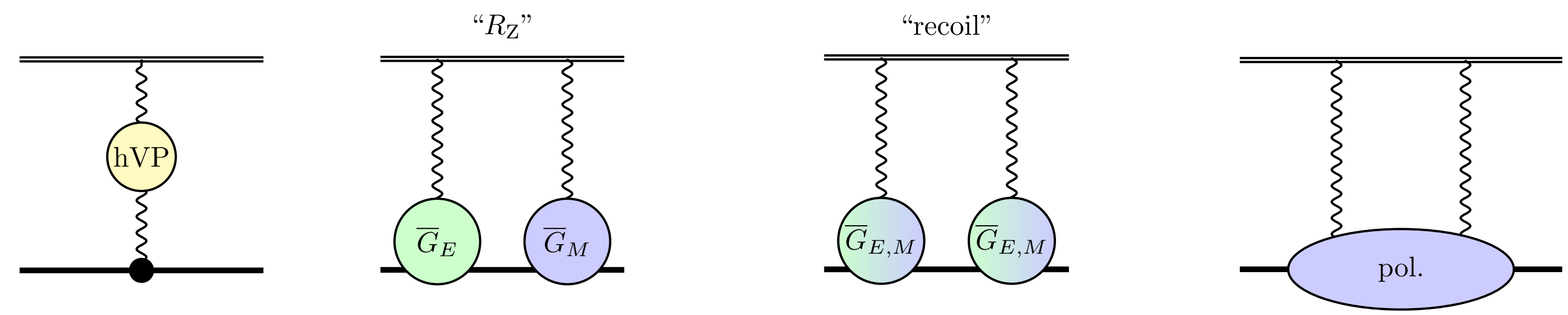

- **Proton-polarizability contribution:**
  - Small discrepancy between BChPT and data-driven predictions remains
- **Finite-size (Zemach radius and recoil) corrections:**
  - Require careful assessment of model uncertainties in form factor input
  - Self-consistent radii extractions from scattering and spectroscopy desired
- **Hadronic vacuum polarization:**
  - Updated results are more precise but also disagree with the existing work
  - Proton finite-size reduces the enhancement of recoil corrections in the HFS

Summary & Conclusions

hadronic = HVP + Zemach radius + finite-size recoil + polarizability

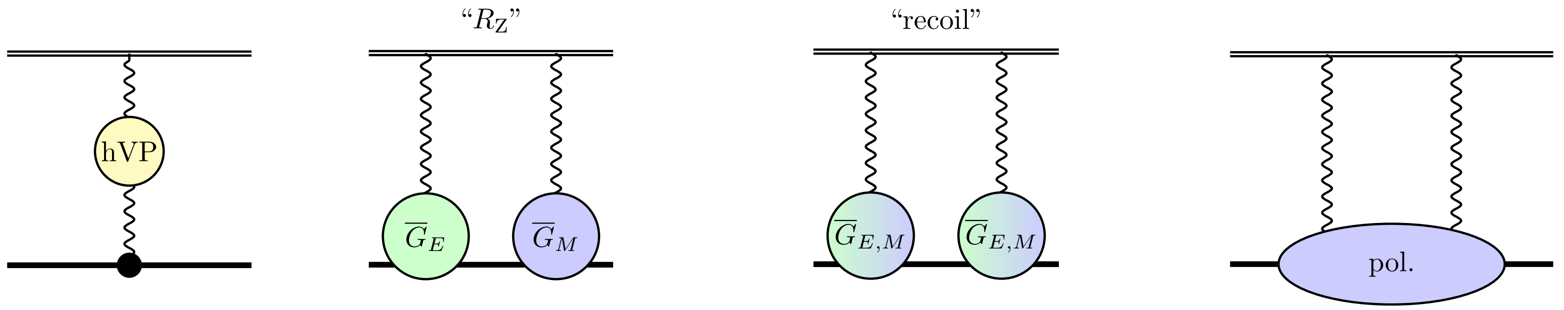

- **Proton-polarizability contribution:**
  - Small discrepancy between BChPT and data-driven predictions remains
- **Finite-size (Zemach radius and recoil) corrections:**
  - Require careful assessment of model uncertainties in form factor input
  - Self-consistent radii extractions from scattering and spectroscopy desired
- **Hadronic vacuum polarization:**
  - Updated results are more precise but also disagree with the existing work
  - Proton finite-size reduces the enhancement of recoil corrections in the HFS
- **Outlook:**
  - Disentangle hadronic effects (e.g., Zemach radius and polarizability contributions) from precise HFS measurements in H and μH

INTERPLAY THEORY ↔ EXPERIMENT

Theory: QED, ChPT, data-driven dispersion relations, ab-initio few-nucleon theories

Experiment: HFS in μH, μHe$^+$, …

Testing the theory

- discriminate between theory predictions for polarizability effect
  - disentangle R_Z & polarizability effect by combining HFS in H & μH
- test HFS theory
  - combining HFS in H & μH with theory prediction for polarizability effect
- test nuclear theories

Determine fundamental constants

Zemach radius R_Z

Interpreting the exp.

extract E^{TPE}, $E^{\mathrm{pol.}}$ or R_Z

Guiding the exp.

find narrow 1S HFS transitions with the help of full theory predictions: QED, weak, finite size, polarizability

Input for data-driven evaluations

form factors, structure functions, polarizabilities

Spectroscopy of ordinary atoms (H, He$^+$)

Electron and Compton Scattering

JG|U JOHANNES GUTENBERG UNIVERSITÄT MAINZ

Hadrons CRC 1660 Nuclei

Cluster of Excellence PRISMA+ Precision Physics, Fundamental Interactions and Structure of Matter

Emmy Noether-Programm DFG Deutsche Forschungsgemeinschaft

Thank you for your attention!

Electromagnetic Properties of Nuclei

Scattering vs. Spectroscopy

Lepton-proton scattering

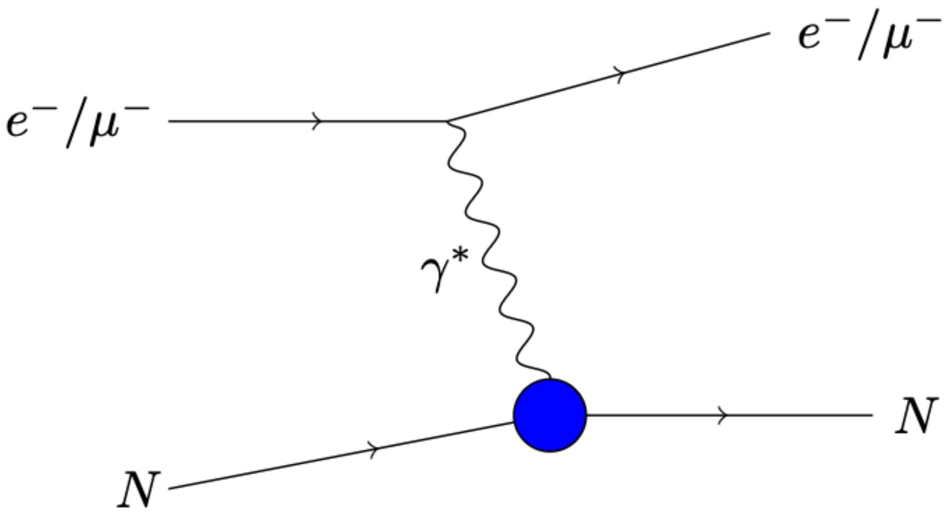

(Muonic)-hydrogen spectroscopy

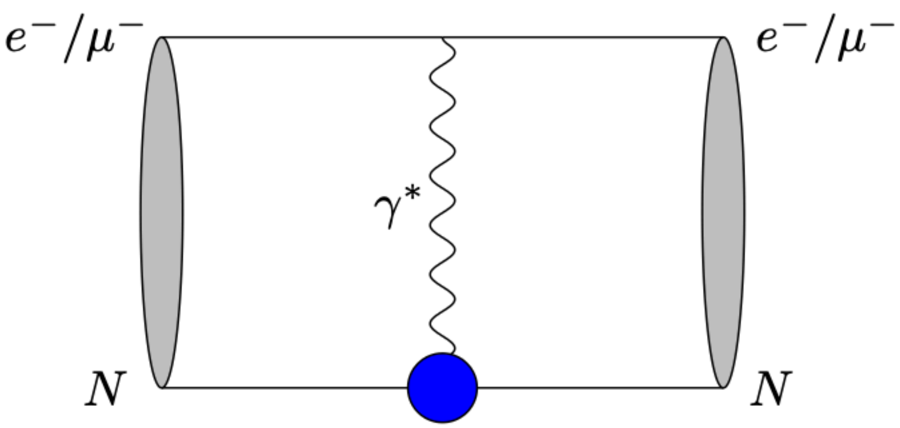

bound-state wave functions

Electromagnetic Properties of Nuclei

Scattering Experiments

- Electromagnetic form factors and structure functions measured in lepton scattering and photoabsorption processes

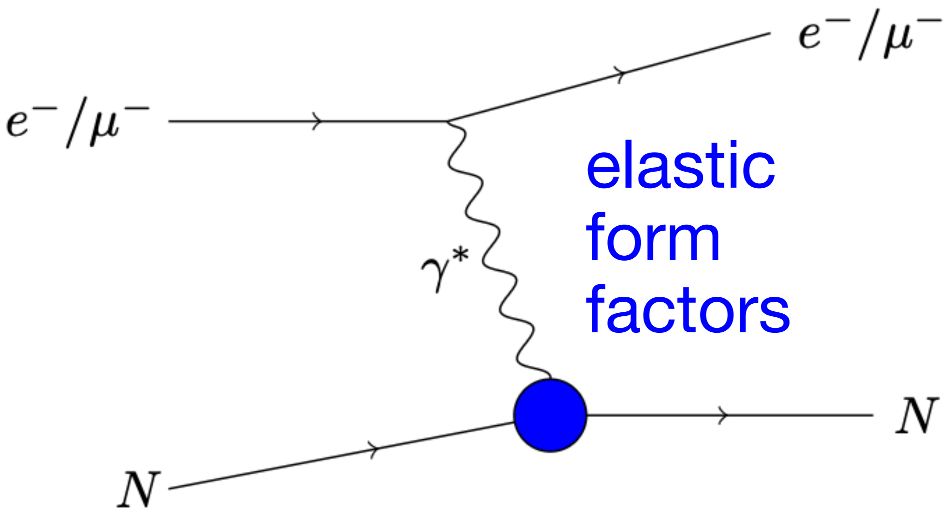

$$\underbrace{\underbrace{\left(\frac{1}{4\pi\varepsilon_0}\frac{Ze^2}{2p_\mathrm{i}c}\right)^2 \frac{1}{\sin^4(\vartheta/2)}}_{\text{Rutherford scattering}} \underbrace{\frac{1}{1+\frac{2p_\mathrm{i}}{Mc}\sin^2(\vartheta/2)}}_{\text{recoil}} \underbrace{\cos^2(\vartheta/2)}_{\text{Spin}}}_{\text{Mott scattering}} \frac{1}{(1+\tau)}\left[G_E^2(Q^2)+\frac{\tau}{\epsilon}G_M^2(Q^2)\right]$$

Electromagnetic Properties of Nuclei

Scattering Experiments

- Electromagnetic form factors and structure functions measured in lepton scattering and photoabsorption processes

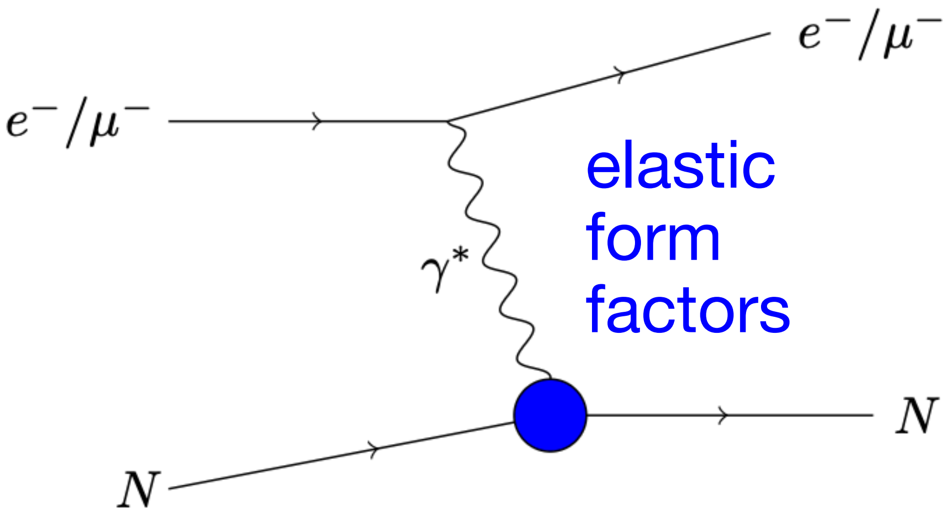

+ radiative corrections …

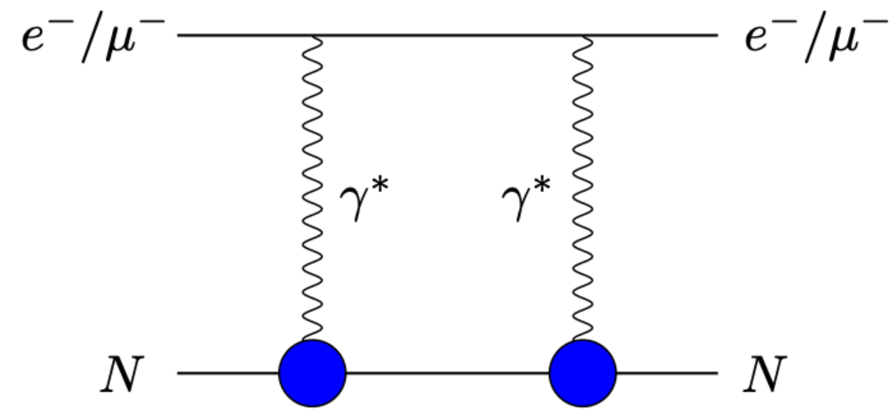

two-photon exchange

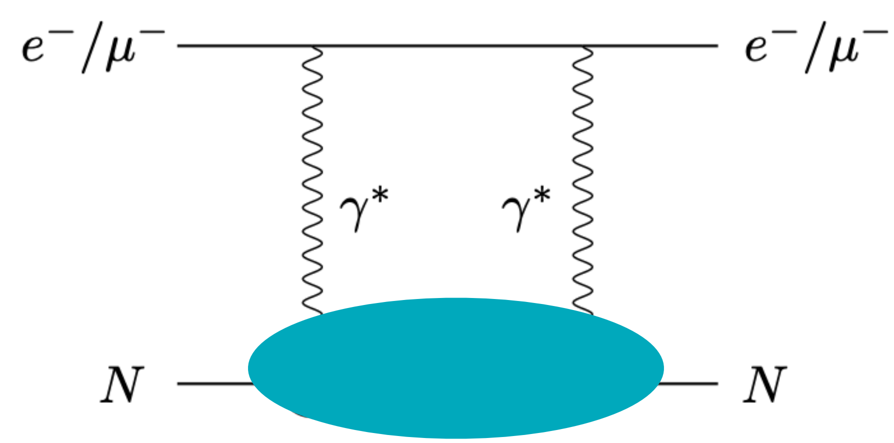

polarizability effect

Electromagnetic Properties of Nuclei

Scattering Experiments

- Electromagnetic form factors and structure functions measured in lepton scattering and photoabsorption processes

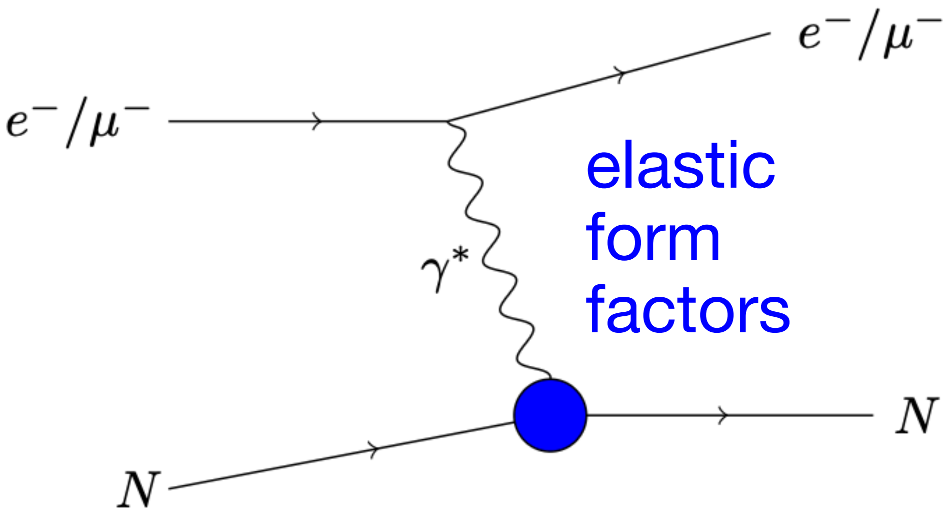

elastic form factors

+ radiative corrections …

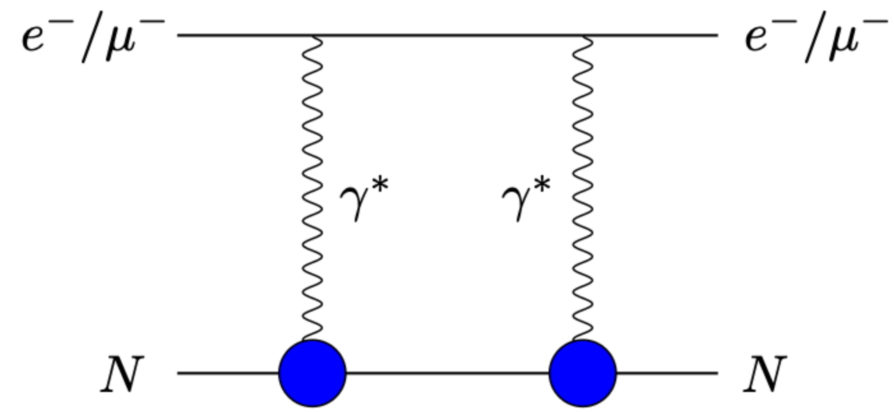

two-photon exchange

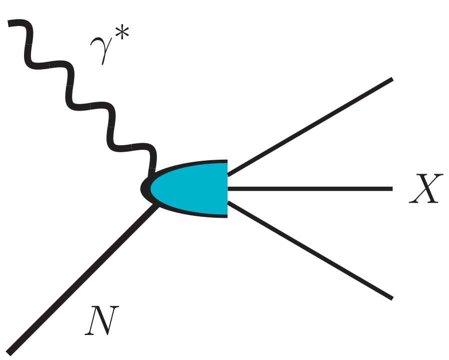

inelastic structure functions

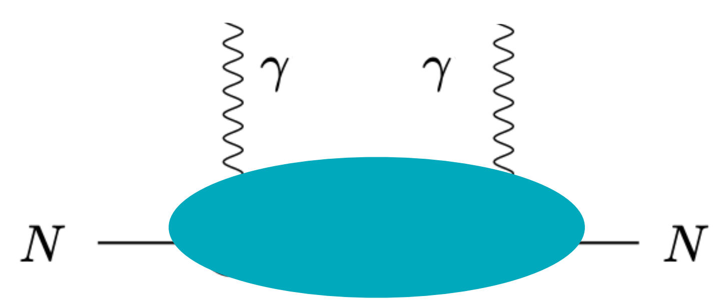

Compton scattering

Proton Charge Radius

Electron Scattering vs. Muonic Hydrogen

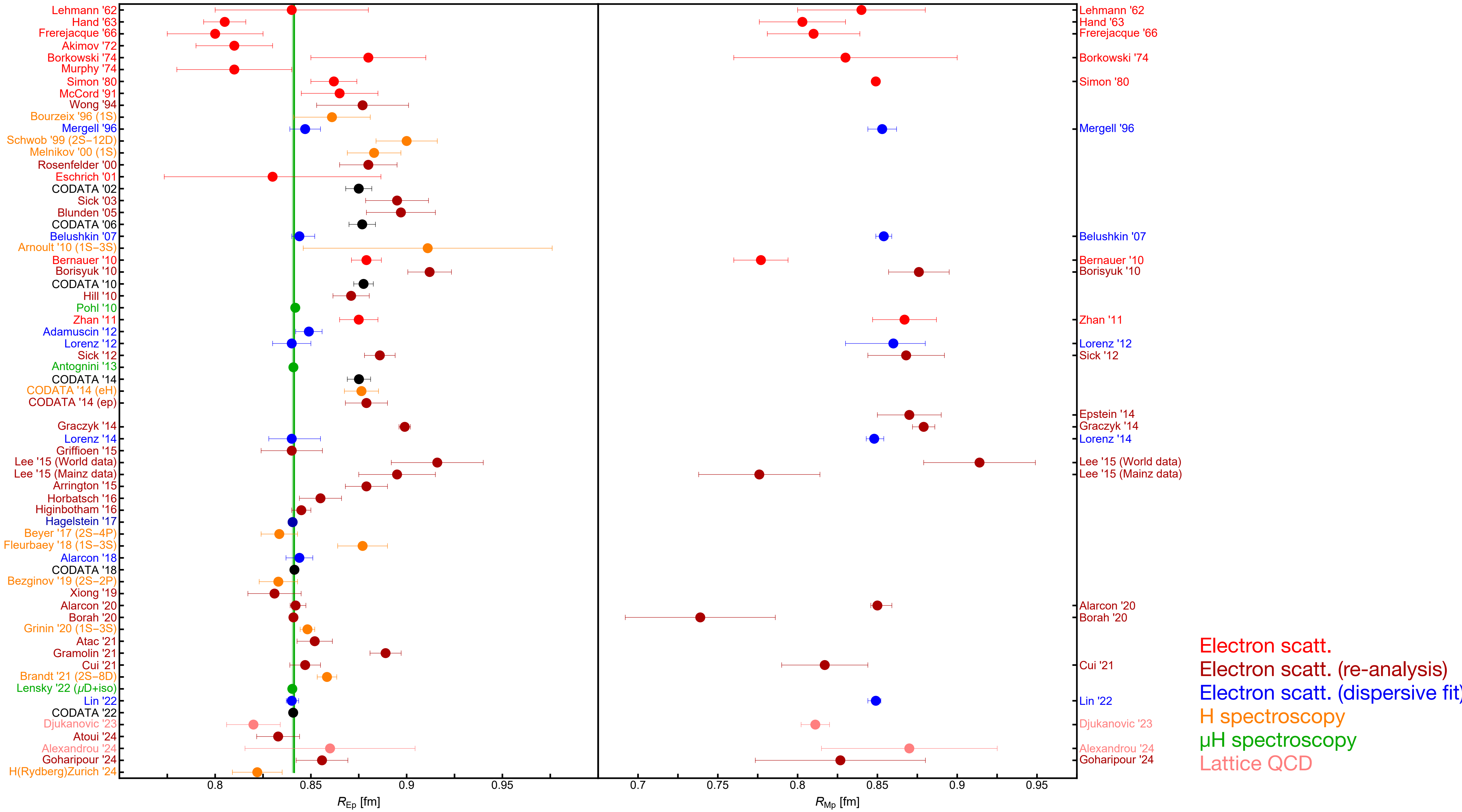

Magnetic Radius Puzzle

Form Factor Uncertainties

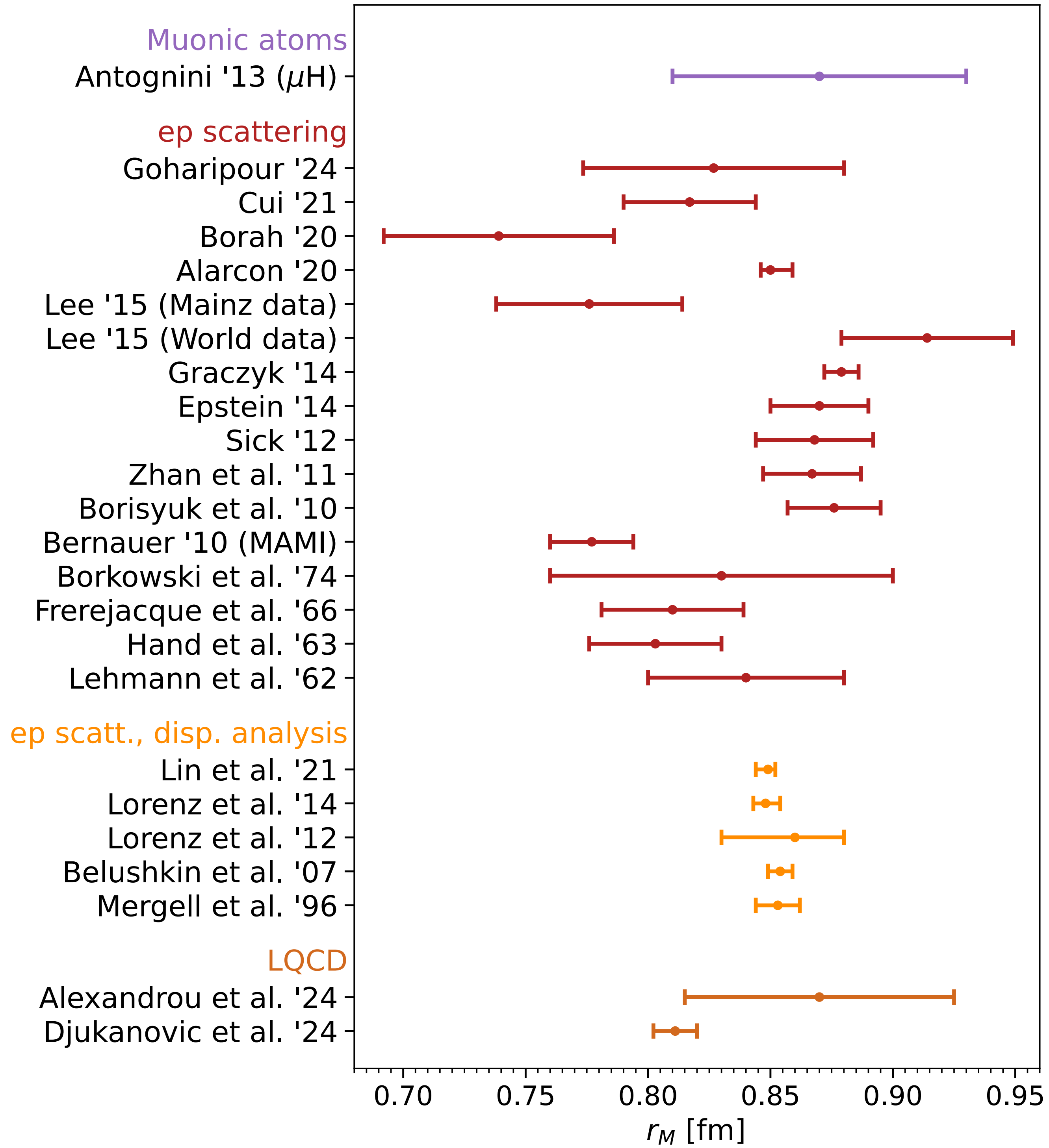

$(Z\alpha)^6$ Finite-Size Corrections

… Limitation of the Finite-Size Expansion

TABLE II: Assessment of the validity of the finite-size expansion in view of the precision requirements imposed by experimental values for the transitions in hydrogen (H), muonic hydrogen (μH) and anti-protonic hydrogen ($\bar{p}$H). We compare the exact un-expanded finite-size effect from Eq. (20) to the finite-size expansion in Eq. (16). The last column presents the difference of the exact finite-size effect and the leading term in the finite-size expansion. For $E_{nl}^{\langle \mathrm{eFF} \rangle}$ in S-, P- and D-levels, we consider the expansion up to and including $\mathcal{O}(\alpha^4)$. For $E_{nS-\mathrm{hfs}}^{\langle \mathrm{mFF} \rangle}$ in the hyperfine splitting, we consider the expansion up to and including $\mathcal{O}(\alpha^5)$.

System	Transition	Experimental Value		Exact Finite-Size Effect (20)	Subleading Finite-Size Effects $\lvert(16)-(20)\rvert/(20)$
H [kHz]	$2S-1S$	2 466 061 413 187.018(11)	[40]	-2.64×10^{-10}	0.002
	$3S-1S$	2 922 743 278 665.79(72)	[41]	-2.91×10^{-10}	0.090
	$2S_{1/2}-2P_{1/2}$	1 057 829.8(3.2)	[42]	3.77×10^{-11}	0.002
	$8D_{5/2}-2S_{1/2}$	770 649 561 570.9(2.0)	[43]	-3.78×10^{-11}	0.002
	$1S$ hfs	1 420 405.751 768(2)	[44, 45]	-1.05×10^{-8}	0.036
	$2S$ hfs	177 556.838 87(85)	[46]	-1.34×10^{-9}	0.017
μH [µeV]	$2P_{1/2}-2S_{1/2}$	202 370.6(2.3)	[37]	-8.08×10^{-10}	0.24
	$1S$ hfs	(0.02)[a]		-1.46×10^{-7}	0.79
	$2S$ hfs	22 808.9(5.1)	[37]	-1.87×10^{-8}	0.74
$\bar{p}$H [keV]	$2P-1S$	8.67(15)	[48]	-1.15×10^{-15}	0.69
	$2S-2P$			-1.40×10^{-16}	0.74

[a] Uncertainty of a future CREMA Collaboration measurement with anticipated 10^{-7} accuracy [38, 47].

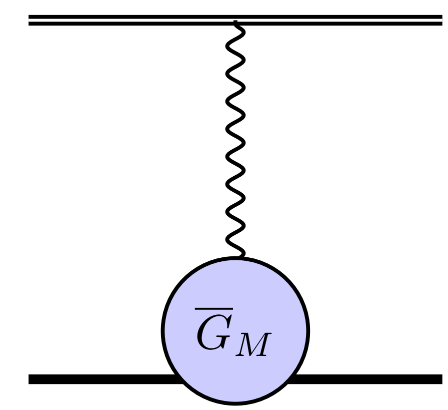

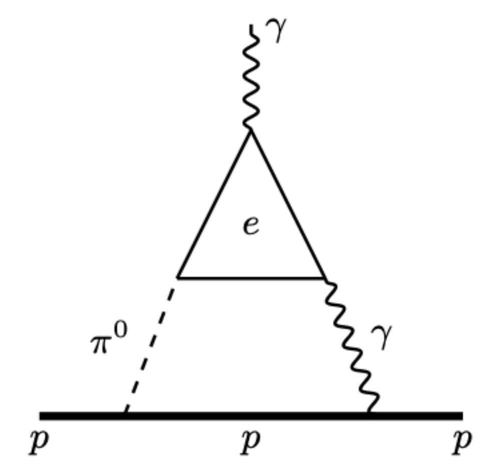

 publication in preparation

TPE Effect in μH Lamb Shift

$$\Delta E^{\mathrm{TPE}}_{nS} = \Delta E^{\mathrm{Born}}_{nS} + \Delta E^{\mathrm{inel.}}_{nS}(\nu_0) + \Delta E^{\mathrm{subtr.}}_{nS}(\nu_0)$$

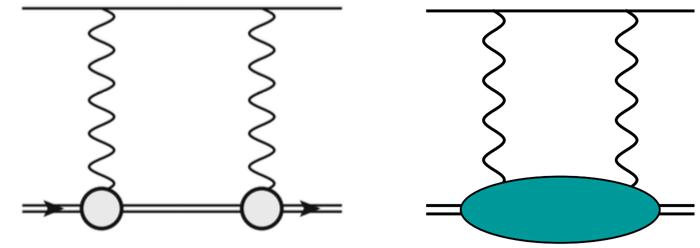

Table 1 Forward 2γ-exchange contributions to the $2S$-shift in μH, in units of μeV.

Reference	$E^{(\mathrm{subt})}_{2S}$	$E^{(\mathrm{inel})}_{2S}$	$E^{(\mathrm{pol})}_{2S}$	$E^{(\mathrm{el})}_{2S}$	$E^{\langle 2\gamma\rangle}_{2S}$
DATA-DRIVEN					
(73) Pachucki '99	1.9	−13.9	−12(2)	−23.2(1.0)	−35.2(2.2)
(74) Martynenko '06	2.3	−16.1	−13.8(2.9)		
(75) Carlson *et al.* '11	5.3(1.9)	−12.7(5)	−7.4(2.0)		
(76) Birse and McGovern '12	4.2(1.0)	−12.7(5)	−8.5(1.1)	−24.7(1.6)	−33(2)
(77) Gorchtein et al.'13 [a]	−2.3(4.6)	−13.0(6)	−15.3(4.6)	−24.5(1.2)	−39.8(4.8)
(78) Hill and Paz '16					−30(13)
(79) Tomalak'18	2.3(1.3)		−10.3(1.4)	−18.6(1.6)	−29.0(2.1)
LEADING-ORDER BχPT					
(80) Alarcòn *et al.* '14			$-9.6^{+1.4}_{-2.9}$		
(81) Lensky *et al.* '17 [b]	$3.5^{+0.5}_{-1.9}$	−12.1(1.8)	$-8.6^{+1.3}_{-5.2}$		
LATTICE QCD					
(82) Fu *et al.* '22					−37.4(4.9)
Fu et al. '24*			−11.7*		−32.2*

$$\Delta E^{\mathrm{TPE}}_{nS} = \underbrace{\Delta E^{\mathrm{Born}}_{nS} - \Delta \mathcal{E}^{\mathrm{Born\ subtr.}}_{nS}}_{=\Delta\mathfrak{E}^{\mathrm{Born}}_{nS}} + \underbrace{\Delta \mathcal{E}^{\mathrm{subtr.}}_{nS} + \Delta \mathcal{E}^{\mathrm{Born\ subtr.}}_{nS}}_{=\Delta\mathfrak{E}^{\mathrm{subtr.}}_{nS}} + \Delta \mathcal{E}^{\mathrm{inel.}}_{nS}$$

*our preliminary results based on their LQCD prediction for $\Delta\mathfrak{E}^{\mathrm{subtr.}}_{nS} = -7.22(81)(57)\,\mu\mathrm{eV}$

CROSS CHECK BETWEEN 3 COMPLEMENTARY APPROACHES

- Data-driven dispersive approach
- Baryon Chiral Perturbation Theory
- Lattice QCD